Elements of Feed-forward and Feedback Control in *Drosophila* Body Saccades

Thesis by

John Andrew Bender

In partial fulfillment of the requirements for

the degree of Doctor of Philosophy

California Institute of Technology

Pasadena, CA

January 2007

Acknowledgments

First, I would like to thank my advisor, Prof. Michael Dickinson. He has been everything a graduate advisor could and should be, demonstrating devoted teaching, mentoring, intellectual curiosity, and scientific and personal integrity, all combined with outstanding research prowess.

I was greatly assisted by now-Dr. M. Reiser with development of the flight arenas used for visual stimulation. Dr. A. Straw designed and built the bulk of the software I used for video data collection. G. Card loaned me the cameras used for the high-speed movies as well as her time to collect those data. Now-Prof. D. Altshuler donated significant time to aid me with statistical analysis. The original idea to tether a fly to a steel pin between two magnets, on which the bulk of this thesis is based, was that of Prof. M. Dickinson. In the end, I physically could not have completed this work without the assistance of L. Shadgett and A. Bender to digitize the halteres in the phase-locked video sequences. Additionally, all of the members of the Dickinson lab have contributed to my intellectual

development, and it was my pleasure to be surrounded by such consistently interesting, entertaining, and enjoyable people. I also appreciate the aid and feedback provided by the members of my committee as this work took shape.

Finally, and most importantly, I would like to express my deepest gratitude to my wife, Amanda. Not only did she work extremely hard in a state of almost complete self-denial for the last *N* years to keep our finances, home, and marriage intact, or even thriving, but she went well beyond her ken and past what anyone could expect by actually helping me to collect data that are included in this thesis. I am proud to be associated with her, and I am a better person for it.

Abstract

I have developed a new experimental preparation of the fruit fly, *Drosophila melanogaster*. A fly is glued to a steel pin, which is held in the field between two magnets such that the fly is free to rotate about only one axis. Such “magnetically tethered” flies perform rapid yaw turns, similar to the behaviors termed “body saccades” in free flight. Saccades can be evoked by visual stimulation, in a manner suggesting that the underlying neural circuitry may be performing an angular threshold calculation. Once a saccade is initiated, however, visual feedback has very little effect on its dynamics, but rotational feedback from the haltere system plays an important role in structuring the time course of saccades. Vision is important, though, in maintaining a stable orientation in both intact flies and flies with asymmetrical wing alterations. The halteres are known to mediate responses to Coriolis forces correlated with the fly's rotations in flight, but flies with modified halteres also exhibit distorted saccade dynamics when they are not free to rotate. This suggests that the halteres may be involved in saccade initiation, although the precise

mechanisms are not clear. There is preliminary evidence suggesting that the haltere strokes may be actively modulated during flight.

Contents

I. Introduction

> Of what use, however, is a general certainty that an insect will not walk with his head hindmost, when what you need to know is the play of inward stimulus that sends him hither and thither in a network of possible paths?
>
> −George Eliot, *Daniel Deronda*

Behavior and internal models

Behavior is the mechanical manifestation of electrical signals in neurons and muscles, at least in organisms complex enough to have neurons and muscles. Therefore, the range of behaviors exhibited by an animal is constrained at the lowest level by the mechanical properties of its body. To the extent to which one can divide the internal functions of an animal into a box diagram, as is common in control-system analyses, such a model might look like the one in Figure I-1. Behavior is the system's output, determined by motor commands played through the physical world. The motor commands are the output of an integrator, instantiated in some fashion by the brain and nervous system. The brain receives sensory inputs from the environment along with estimates of the animal's internal states (hunger, mating status, etc.) and computes an appropriate motor output. Efficiency and coevolution probably dictate that the nervous system

is implicitly tuned to receive sensory input in the ranges most likely to be encountered in the real world and to produce motor outputs that correspond to physically possible, coordinated movements.

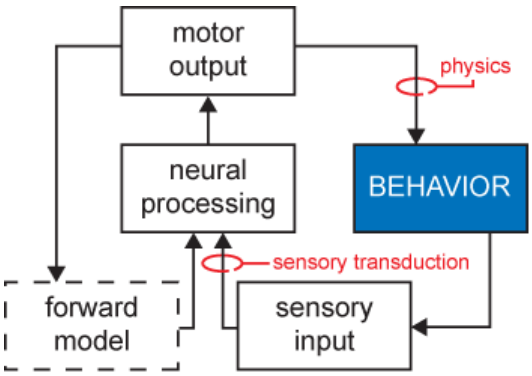

Figure I-1: A box diagram including some of the factors influencing what we observe as behavior. The system is presumably adapted to the ranges of sensory inputs and physical constraints (indicated in red) that are most likely to be encountered in nature. The existence of forward models is generally speculative, but comparing the actual sensory input with the output of such a model, rather than with a desired, fixed point in sensory input space, could improve the speed and reliability of behavior.

However, a system designed to minimize the error between the planned and actual effects of a motor pattern, as measured by the difference between expected and received sensory input, can become unstable in the face of delays, such as those introduced by muscle contraction or sensory transduction. An example of this is an animal attempting to orient toward a sensory stimulus. If the "desired" sensory input state is one in which the stimulus is directly in front of the animal, any other inputs will lead to an appropriate turning response. However, because of the delays between the animal's motion and its perception of that motion, by the time it receives sensory input indicating that the stimulus is in front of it, the animal will have continued turning past the desired orientation, and the termination of the turning behavior takes additional time. Depending on the strength of the response and the introduced delays, this could produce unstable oscillations about a desired orientation, rather than a robust fixation response. One way to compensate for this problem is to reduce the feedback gain, such that the animal approaches the desired orientation very gradually, but this might

not be a good solution for all problems. Another hypothetical solution involves the use of an explicit model of the muscles and external forces to anticipate future sensory information, comparing incoming sensory input to the output of this model rather than the final, desired sensory input. Such a “forward model” would allow a faster and more robust response, and is a common engineering solution. The questions of existence and probable mechanisms for biological implementations of forward models have been treated extensively, with inconclusive results (Miall and Wolpert, 1996; Kawato, 1999; Mehta and Schaal, 2002; Karniel, 2002; Webb, 2004). Another possibility is that motor commands could be planned and executed without any reference to their actual effects. Such feed-forward motor plans may be useful for actions that are very rapid or stereotyped and are therefore unlikely to be altered in response to external perturbations. However, the very availability of sensory feedback seems to make it unlikely that additional information, however minimal or noisy, would not be utilized to reduce the error between the planned and actual outcome of a motor pattern. Whether or the degree to which nervous systems actually do so remains an open question, with the answer expected to vary based on the animal, the specific behavior, and possibly the animal's internal states and experiences.

Saccades

One behavior for which sensory feedback could conceivably be neglected without significant consequences is the saccade. In humans, saccades are very rapid movements of the eyes, famously noted by Yarbus (1961; 1967). Between saccades, the gaze is actively stabilized at a constant point (Walls, 1962). One

function of saccades in primates is thought to be synthesizing a high-resolution view of the world by scanning large areas of the scene with the spatially limited fovea. However, the phenomenon of stable gazing interspersed with rapid changes in eye direction has been observed in animals across three phyla, an extreme example of evolutionary conservation or convergence (see the excellent review by Land, 1999). Saccades are exhibited not only by animals which do not have foveas, but in animals in which the eyes cannot be rotated independently of the head. In such animals, one primary function of saccades is thought to be the reduction of image blur, caused when an area of the image moves from one photoreceptor to another faster than each photoreceptor can process the image (Land, 1999).

Rotation of a fluid-filled sphere (e.g., an eyeball) is a mechanically simple process, and eye saccades by primates take place over tens of milliseconds (Jürgens et al., 1981). Therefore, as the error between the planned effects of the saccadic motor commands and the actual endpoint of the eye's rotation is very likely to be small, it may be reasonable to perform these behaviors without the integration of ongoing sensory feedback. Because phototransduction also takes tens of milliseconds (Hartline, 1934; Fuortes and Hodgkin, 1964; French, 1980), visual feedback is only available to compare with the expected retinal image after a delay comparable to the duration of the entire behavior and is therefore unlikely to be useful in modifying the motor pattern (Jürgens et al., 1981). However, there is evidence that saccades can be influenced by feedback from other sensory

modalities such as the vestibular system (Morasso et al., 1973; van Opstal and Kappen, 1993; Fukushima and Kaneko, 1995; Ramat et al., 2007) that can respond much more rapidly to changes in sensory inputs.

Saccades in Drosophila

Because the compound eyes of flies are fixed relative to the head, saccades generally occur as rapid rotations of the entire body, and were therefore termed “body saccades” by Land and Collett (1974). Flight in the fruit fly, *Drosophila melanogaster*, is characterized by segments of relatively straight flight and rapid, saccadic turns (Tammero and Dickinson, 2002a), described earlier in other fly species (Land and Collett, 1974; Wagner, 1986; Schilstra and van Hateren, 1999). These changes in heading take place over tens of milliseconds (Schilstra and van Hateren, 1999; Fry et al., 2003) and can also include rotations of the head consistent with additional gaze stabilization during the body turn (Land, 1973; van Hateren and Schilstra, 1999). Observing *Drosophila* flying around an arena with 1 m diameter, Tammero and Dickinson reported that saccades have a distribution of amplitudes centered around ±90° (Tammero and Dickinson, 2002a). One way that saccades can be elicited is through visual expansion, which triggers a saccade in the opposite direction once the summed expansion to one side of the fly exceeds a certain threshold (Tammero and Dickinson, 2002a). This threshold can be modulated by other cues, such as the presence of an olfactory stimulus (Frye and Dickinson, 2004a).

Flies tethered for experimental tractability also perform body saccades, which are exhibited as short bursts of turning torque in one direction or the other

(Heisenberg and Wolf, 1979). However, the duration of saccades in tethered flies is more on the order of 500 ms than the 50 ms observed in free flight, and unrestrained flies must generate both torque to start turning and countertorque to stop, but tethered flies never generate countertorque (Fry et al., 2003; Heisenberg and Wolf, 1979). This raises the question of whether the behaviors observed in tethered flies are truly saccades, in the neurobiological sense, or are generated by an unrelated motor program. Flies which were loosely tethered, using a string and a magnet which allowed them to rotate freely about their yaw axis, also performed stereotyped turns with a time course more closely resembling that observed in free flight (Heisenberg and Wolf, 1984; Mayer et al., 1988). However, these investigations explicitly failed to find a visual stimulus which could reliably evoke these turns.

Because the dynamics of flapping flight are much more complicated than the rotation of an eyeball, it is unlikely that body saccades are generated with a purely feed-forward motor program, especially given that even primate eye saccades do not appear to be. This gives credence to the idea that saccades in free flight and tethered flight are, in fact, the same behavior, modified by the differences in sensory reafference between the two conditions. Although this experiment has not been done, recording torque during a saccade in tethered flight would be comparable to recording from the muscles responsible for actuating an eyeball that was not free to rotate during a saccade. It seems likely that the observed time course of muscular contraction would be substantially different in such a case.

The halteres and multimodal sensory integration

Somewhat analogous to the primate vestibular system, the true (dipteran) flies possess specialized sense organs called halteres (Figure I-2). The halteres beat in antiphase to the wings during flight, and function as gyroscopes, sensitive to the angular velocity of the fly about any arbitrary axis (Fraenkel and Pringle, 1938; Pringle, 1948; Nalbach and Hengstenberg, 1994; Nalbach, 1994). Flies are known to respond quickly and robustly to haltere-mediated rotational stimulation (Fayyazuddin and Dickinson, 1996; Dickinson, 1999; Sherman and Dickinson, 2003). Therefore, just as the vestibular system provides primates with rotational feedback information during saccades, it may be that feedback from the haltere system is responsible for the differences between tethered and free-flight saccades.

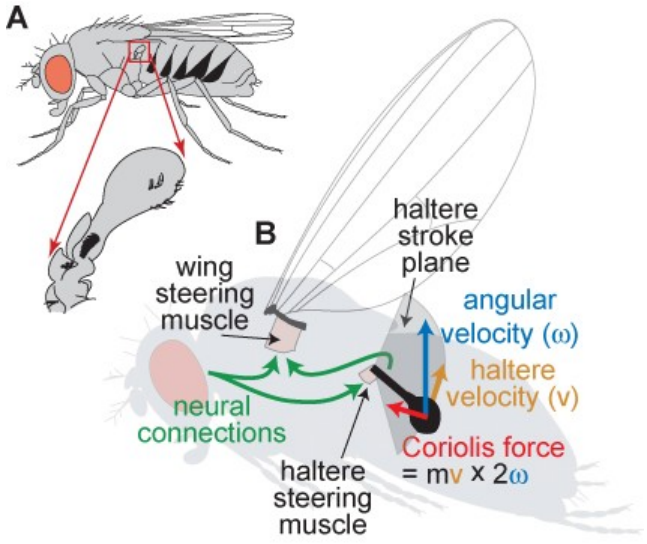

Figure I-2: (A) Haltere. **(B)** The Coriolis force is the cross-product of the haltere's momentum and the angular velocity of the fly, acting to deflect the haltere from its stroke plane. Mechanoceptors near the base of the haltere convey information about the haltere's deflection to the wing steering muscles. Descending visual input can drive both the wing steering muscles and the haltere steering muscles.

Tammero and Dickinson demonstrated that tethered flies stimulated with visual expansion perform turns away from the stimulus, comparable to the responses seen in free flight (Tammero and Dickinson, 2002b). However, even when tethered flies were free to control the position of the visual panorama by

modulating their wingstroke kinematics, the duration of these turns was still an order of magnitude longer than during free flight. Just as in primates, though, an entire saccade takes place on a time scale similar to that required for phototransduction and a visually mediated flight response (estimated at 30 ms in *Musca* by Collett and Land, 1975). The frequency-response characteristics of the halteres and visual system in *Drosophila* show a decrement in the response to visual rotations but robust haltere-mediated reactions to the range of rotational frequencies experienced during saccades (Sherman and Dickinson, 2003). Feedback from the halteres and the visual system is combined in a weighted sum by the flight control circuitry, with a greater emphasis placed on haltere-mediated feedback (Sherman and Dickinson, 2004). These results suggest that naturalistic feedback from the halteres may play an important role in shaping the output of saccade motor program.

The present contribution

Here, I have developed a novel behavioral paradigm, based on the loose tether described by Heisenberg and Wolf (1979; 1984; Mayer et al., 1988). A fruit fly, *Drosophila melanogaster*, is tethered to a steel pin, and the pin is held in the field between two magnets such that it is free to rotate about only one axis. This allowed a “magnetically tethered” fly to control its own orientation with closed-loop feedback from both the visual system and the halteres, in the absence of experimental manipulations. I monitored the fly's heading in real time using a mirror and camera. Around the fly, I placed a cylindrical arena formed of light-emitting diodes (LEDs) which were controlled by a computer which was also

monitoring the output of the camera. Using this new apparatus, I presented flies with controlled visual stimulation, demonstrating that body saccades can be evoked by expanding objects in a manner consistent with an angular threshold detection circuit. Altering the visual and haltere-mediated feedback received by flies while they were performing saccades revealed that visual rotation has only a minor effect on the time course of saccades, while feedback from the halteres plays a strong role. Examination of the halteres of rigidly tethered flies indicated that they may be actively modulated during flight, but the mechanisms and consequences of this have yet to be determined.

Some of this work has previously been published separately (Bender and Dickinson, 2006a; 2006b), and other parts may be published in peer-reviewed journals at a later date. The movies referenced, in addition to high-resolution and vector-graphics versions of the figures, are available from http://mosca.caltech.edu/~jbender/thesis/ , or by clicking on the links in the text and on the figures themselves.

II. Flight on the Magnetic Tether

Chapter Contents

Stocks and Tethering

For all experiments, I used female fruit flies, *Drosophila melanogaster* Meigen, from a laboratory culture descended from 200 wild-caught females. I took 3- to 5-day-old flies from this stock and cold-anesthetized them using a Peltier stage maintained at about 4°C, holding the fly to a mounting stage using light suction. Next, I applied a small amount of UV-activated adhesive (Loctite, loctite.com) to the blunt end of a steel insect pin with a nominal size of 0.1 mm but an actual diameter closer to 50 µm (Fine Science Tools, finescience.com). The pin was held by a ball of putty to a micromanipulator arm, which I maneuvered until the pin was held with its blunt end positioned at the anterior surface of the fly's notum. Finally, I cured the adhesive using a UV light gun, taking care to allow the fly's head and neck to remain separate from the pin and

thorax. This left the pin projecting upward and forward at about a 45° angle from the fly's back, equivalent to the angle of attack made by the fly's body during forward flight (David, 1978; Fry et al., 2003).

On two groups of flies I clipped away a large portion of the surface of one of the wings using dissection scissors – either the posterior half of the right wing or the distal third of the left wing (Figure II-1). These ablations caused a large asymmetry in the aerodynamic forces generated by the wings in flight, and many flies treated in this manner could not sustain free flight. As a rule, only experimental data from flies which maintained flight in the flight arena for 10 min or longer were analyzed.

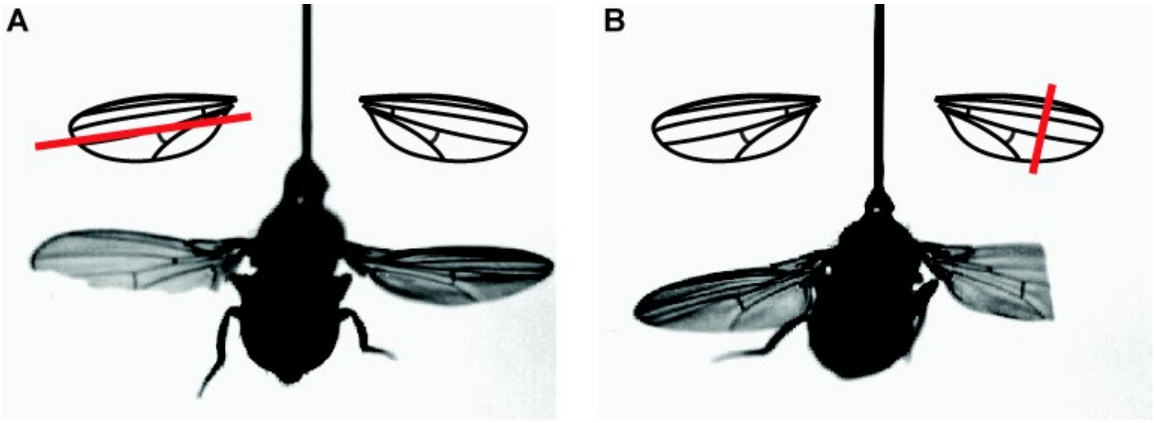

Figure II-1: One high-speed video frame of two magnetically tethered, wing-clipped preparations, both facing the camera. **(A)** The posterior half of the right wing was removed. **(B)** The distal third of the left wing was removed.

The Magnetic Tether

Configuration and considerations

The “magnetic tether” arena was a new experimental apparatus developed for these investigations. Based on an idea first published by Heisenberg and Wolf (1979), in which they credit the concept to E. Buchner, a fly is held fixed in place

but left free to rotate about one axis through the application of a magnetic field. Heisenberg and Wolf achieved this by gluing a small piece of metal to the fly's back, attaching a long, thin thread to the metal, and placing the “loosely tethered” fly above a conical magnet. The metal and fly were therefore held in place by the magnet, but were free to rotate about an axis parallel to the thread. They monitored the fly's orientation using an infrared light source and a photodiode which was occluded by the fly's abdomen as it rotated, and the thread was actively spooled by a motor coupled to the fly's rotation in order to minimize the torsional force imparted due to twisting of the string (Heisenberg and Wolf, 1984; Mayer et al., 1988). The device I built was somewhat simpler. I glued flies to standard insect pins as described above, and used a pair of vertically aligned, rare-earth (NdFeB) magnets (K&J Magnetics, kjmagnetics.com), ~5 cm apart, to hold the pin in place (Figure II-2). The sharp end of the pin rested in the V-shaped aperture of a sapphire bearing (Small Parts, smallparts.com), which was fixed to the center of the upper magnet.

In this situation, the forces acting on the pin come from three sources: the magnetic field, the fly, and gravity. The two vertically aligned magnets produce a magnetic field much as if they were one continuous magnet, except for a slight outward bowing deformation in the empty space. Thus, the field lines are generally vertical in the vicinity of the fly. The pin is held strictly parallel to the field lines as it becomes magnetized, and the magnetic field forces act on the iron in the pin and are therefore

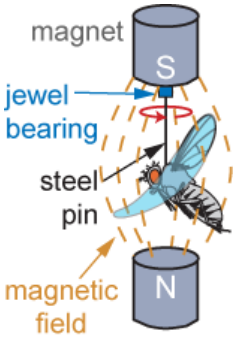

Figure II-2: A fly on a magnetic tether. The pin is held vertically in the magnetic field (represented by the orange lines), but is free to rotate in the bearing, about its long axis.

proportional to the mass of the pin. The magnetic field acts like a spring, resisting movement away from the resting state with a roughly position-dependent restoring force. However, if the pin is pushed too far from the vertical, the attractive force of the north pole of the upper magnet grows larger than the restoring force from the north pole of the lower magnet and the pin is forced away from the vertical until it rests horizontally on the lower surface of the upper magnet. Therefore, there are three equilibria for the pin: a vertical position, aligned with the two magnets; a horizontal position, acting almost solely under the influence of the top magnet; and an unsteady equilibrium at some angled position where the upper and lower magnets affect the pin's induced south pole equally.

The angle of the stroke-averaged force vector produced by the fly is fixed relative to the body (Vogel, 1966; Götz, 1968), and so a free fly accelerates much like a helicopter, by changing its body angle of attack. Therefore, it is common to refer to the fly's yaw, pitch, and roll axes in functional terms, relative to its flight path, rather than with strict reference to the fly's anatomy (after Dickinson, 1999). A fruit fly is capable of generating pure rotation about its functional yaw axis, but turns are frequently banked, including rotations about the functional yaw, pitch, and roll axes (Fry et al., 2003). On the magnetic tether, the fly cannot move along the long axis of the pin, so all aerodynamic maneuvers other than pure yaw rotation result in a torque perpendicular to the pin, i.e., across the magnetic field lines. Although the magnetic field partially damps these forces, when the fly is flying particularly vigorously or the pin is especially long or thin, the fly can induce a noticeable deflection of the pin away from the vertical, oscillating as its

aerodynamic force moments phasically act across the magnetic field lines. Using a thin pin minimized added rotational inertia, proportional to $\frac{1}{2}mr^2$ where m is the mass of the pin and r is its radius, so increasing the magnetic force by using a larger pin was not desirable. Therefore, I cut one-third to one-half off the length of the pins before tethering, reducing the moment arm about which the fly could produce cross-field torque. Another solution I utilized was to strengthen the field from the lower magnet by increasing its mass and moving it as close as possible to the fly, with the caveat that a large, stationary object close to the fly could affect its behavior.

Torque and intrinsic body properties

Historically, it was thought that the aerodynamics of flight in small insects, such as *Drosophila*, was dominated by the viscosity of air, and thus by friction (Reichardt, 1973; Reichardt and Poggio, 1976). Specifically, the time constant of the system, defined as the ratio of the inertial effects to frictional effects, had been estimated as low as 0.02 s by earlier investigators (Mayer et al., 1988). However, Dickinson and co-workers (1999) developed a dynamically scaled robot to measure the forces produced by flapping wings, and Fry and colleagues (2003) used this device to show that inertia is a major component of the forces acting on an unrestrained fruit fly. This analysis hinged on a large value of 1 s for the time constant (I/C), based on detailed estimates of the fly's moment of inertia ($I = 5.2 \times 10^{-13}$ Nm·s^2) and coefficient of friction ($C = 5.2 \times 10^{-13}$ Nm·s) from body morphology. These estimates translate only partially to magnetically tethered flies, because the magnetic tether introduces both additional frictional damping

and rotational inertia. Because of the aerodynamic regime in which fruit flies operate, a slight shift in the balance between friction and inertia could have large effects on the constraints of behavior, particularly for behaviors such as saccades which take place over 50–70 ms in free flight (Fry et al., 2003).

The gravitational force acting on a magnetically tethered fly was generally very small relative to the magnetic field and the fly's own force production, but I made use of gravity to estimate the relative contributions of inertia and friction to the yaw rotation of the fly. I tethered several flies and then killed them by freezing, and slightly misaligned the magnets such that the weight of the fly's abdomen introduced a preferred orientation of the dead fly within the arena. I blew gently on the fly to make it rotate and recorded the oscillations as it returned to its preferred orientation (ϕ=0). I fit the time course of these observations with a damped, spring-mass oscillator function of the form:

$$I\ddot{\phi} - C\dot{\phi} = K\phi \quad , \tag{II-1}$$

where I represents the fly's moment of inertia, C, its coefficient of rotational friction, and K, the spring constant, which is determined by gravity and the magnetic field. I fit these constants by sequentially calculating the fly's angular velocity and acceleration from the time course of its orientation, using iteratively estimated values for the constants which minimized the mean-squared error between the model and the data for each trial (sample traces shown in Figure II-3). The inertia and friction calculated by this method are relative to the precise value of K, but the ratio I/C is independent of K. Termed the time constant of the system, this ratio describes the relative effects of viscous and inertial forces on

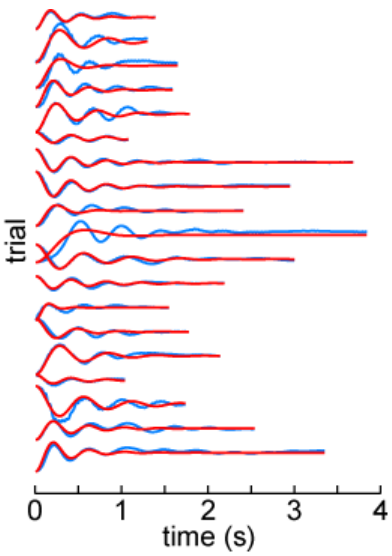

Figure II-3: Damped oscillations caused by gravity acting on a dead fly in a nonvertical magnetic field. Blue traces: fly's orientation; red traces: model fit to data by estimating values of inertia, friction, and tension (gravity) that minimized the mean-squared error for each trial.

the fly. The values I derived for these constants include all added effects of the tethering apparatus, in addition to the purely aerodynamic measures. The moment of inertia of the pin about its long axis was on the order of 10^{-15} Nm·s^2, less than 1% of the fly's moment of inertia about its yaw axis (Fry et al., 2003, Mayer et al., 1988). However, the fly was not rotating about its center of mass, but rather about the pin. I estimated that the tethering point was offset from the end of the fly by one-sixth of the body length, and calculated the inertial effects of this altered center of rotation on a model cylinder. A cylinder with the fly's approximate size (mass=1.25 mg, radius=0.4 mm, length=2.5 mm) and moment of inertia, 5.2x10^{-13} Nm·s^2 (Fry et al., 2003, based on body morphology), rotated about this point rather than its center, has an almost precisely doubled moment of inertia. Other than body drag, added friction is introduced by of the sharp end of the pin rotating against the sapphire bearing.

This method yielded average time constants of 0.19±0.03 s for flies with raised wings and 0.43±0.13 s for flies with folded wings, both values still much longer than the duration of a saccade (Figure II-4). I then estimated the torque (T_ϕ) produced during a saccade from a dynamic model governed by the equation:

$$T_\phi = I\ddot{\phi} + C\dot{\phi} \quad , \qquad \text{(II-2)}$$

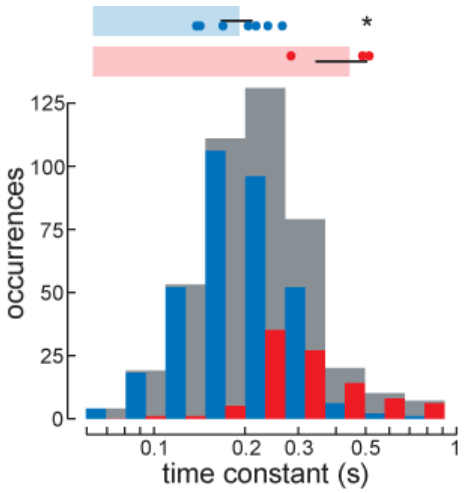

Figure II-4: Time constant (*I*/*C*) for passively rotating flies in a misaligned magnetic field. Blue: flies with wings raised (N=7 flies); red: flies with wings folded (N=3). Horizontal bars at top show mean time constant across all flies of each type; black line indicates the s.e.m; dots denote the mean time constant for each single fly (*: $p<0.05$). Histograms show best-fit time constant for all trials, color-coded by the fly's wing position (gray = sum of red and blue bars; n=338 trials with wings raised; n=97 with wings folded).

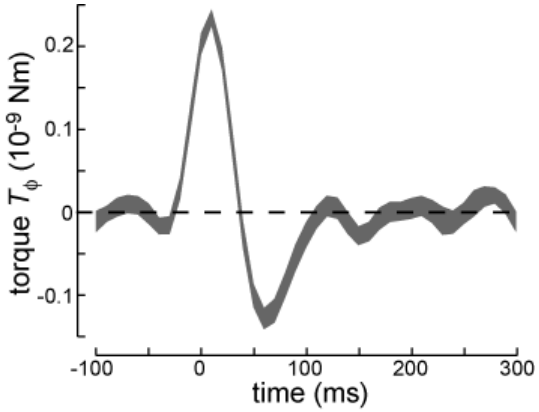

Figure II-5: Estimated time course of torque production during saccades by magnetically tethered flies, using a time constant of 0.2 s. The envelope indicates the s.e.m. (n=87 saccades). Estimates made using time constants of 0.4 or 1 s overlap almost completely with the data shown.

where ϕ is the recorded time course of the fly's orientation. Using saccades with amplitudes ranging from 24.25–25.75° and peak angular velocities from 490–510°·s^{-1} (see Figure III-9), and the lowest-valued time constant (*I*/*C* = 0.2 s), I found that magnetically tethered flies produce significant countertorque at the end of saccades, indicating that they must overcome inertial forces in order to stop turning (Figure II-5).

Magnetic tether arena

Around the arrangement of the two vertically aligned magnets, I formed a cylindrical arena from panels of 8x8 LEDs, totaling 32x64 green LEDs around a volume measuring 8x13 cm, each LED subtending about 5.6° of azimuth. This compares well with the average interommatidial spacing of 4.6° in the *Drosophila* eye (Götz, 1964; Egelhaaf et al., 1989). The LEDs were refreshed at 800 Hz to remain well above the estimated 200 Hz flicker-fusion rate of the fly (Autrum,

1958; Laughlin and Weckstrom, 1993), and the contrast was always at the maximum possible for the display (Reiser, 2006). For most experiments, the pattern displayed on the LED panels was updated at 50 Hz. Display commands were issued from an associated control board (Reiser, 2006; Reiser and Dickinson, in press), which in turn was controlled by an attached Linux PC running custom software in the languages C and Python.

The fly was illuminated with a circular array of near-infrared (940 nm) LEDs placed around the lower magnet. Although the fly's visual system is insensitive to this wavelength (Stark and Johnson, 1980), the light reflected from the fly's light-colored ventral side was passed by a mirror to an infrared-sensitive camera (A602f, Basler, baslerweb.com) positioned above the arena (Figure II-6). The camera, collecting at 101 Hz, was attached to the same PC which was responsible for outputting the arena display commands. After I tuned the image threshold by hand for each fly to produce white images of the fly on a black background, software on the PC extracted the orientation of the fly in real time (within 3.5 ms after image collection) for each frame and saved it to disk for further analysis. I estimated the uncertainty of the orientation derived from this method by tracking a stationary, dead fly for 1 h. The standard deviation of the fly's orientation under these conditions was 1–2°, which

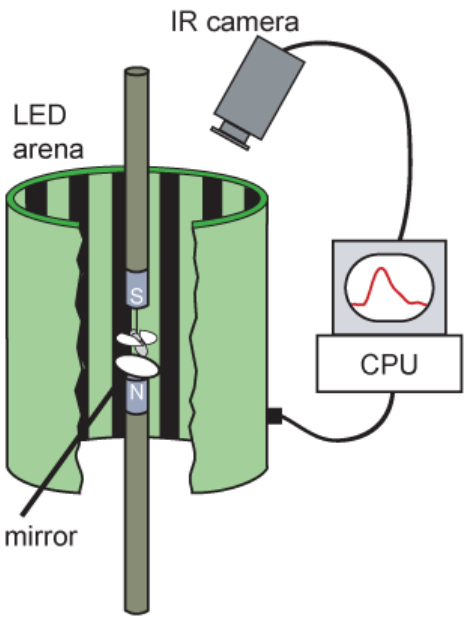

Figure II-6: Magnetic tether arena.

should be representative of the tracking error during the experiments. The shutter speed of the camera was set to 1.7 ms, about one-third of a wingstroke, so the wings were not visible and did not add to the tracking error (see Movie II-1). An additional source of error was introduced by the fact that the relative positions of the camera and the visual arena varied slightly from animal to animal because of the necessity of moving them to insert and remove flies from the apparatus. I estimate that this error is on the order of ±5°, limiting only my ability to determine the relative orientation of the stimulus and the fly.

Since the silhouette of a fly carries little information to differentiate head from tail, I initiated a calibration sequence to disambiguate the orientation of the fly within the arena before beginning an experiment. The arena displayed a horizontal square wave grating with a fundamental spatial frequency of 45°, corresponding to individual stripe widths of 4 pixels. I shifted the pattern in opposite directions in two halves of the arena at $300°\cdot s^{-1}$, creating a pole of visual expansion and a pole of visual contraction, separated by 180°. Flies vigorously attempt to maintain the pole of contraction at a frontal position under such conditions (Tammero et al., 2004; Reiser, 2006). I rotated the poles around the arena at $120°\cdot s^{-1}$, inducing the fly to spin in circles for 1 min. Because the fly's center of mass was offset from its center of rotation, the time course of the position of the fly's visual center described a circle. This allowed the software to unambiguously determine in real time which way the fly was facing, using the current position of its visual center relative to the recorded center of rotation.

A group of flies was tested for stable flight in total darkness. Although the room lights were off during all experiments, for these I also covered the arena and camera with a sheet of thick, black fabric to eliminate as many potential visual cues as possible. The luminance inside the arena was measured at <0.1 lux under such conditions. The arena alternated, in 1-min periods, between darkness and the display of a static pattern, which both provided an internal control and served to minimize dark adaptation (Bernhard and Ottoson, 1960). Since flight duration is known to be reduced under conditions lacking closed-loop visual stimulation (Heisenberg and Wolf; 1988; Dickinson, 1999), I included data from flies which flew continuously for 5 min or more in these experiments.

Stability on the Magnetic Tether

Flies with their wings clipped asymmetrically are capable of maintaining straight flight on the magnetic tether. Using a detailed mathematical model of the aerodynamics of flapping flight (Dickson et al., 2006), I simulated the effects of similar wing modification on the stroke-averaged forces generated by the model wings. If the flies did not alter their wingstroke kinematics, clipping either the distal third of the left wing or the posterior half of the right wing would lead to the production of a significant yaw moment. The direction of this predicted moment was the same for both treatments (i.e., they would both tend to turn counterclockwise). This is supported by the observation that when I cut away too much wing surface in some preparations, they spun uncontrollably on the magnetic tether, and flies with both treatments spun in the same direction. The

magnitude of the predicted yaw moment was similar for both modeled wing modifications ($3x10^{-3}$ $mg \cdot mm^2 \cdot ms^{-2}$), suggesting that I may have empirically arrived at the maximum stroke-averaged yaw moment which the flies were capable of compensating.

I recorded high-speed video sequences (6000 $frames \cdot s^{-1}$) of both types of modified flies while they were flying with a constant heading (Movies II-2 and II-3). Flies with the distal part of the wing removed exhibited a marked asymmetrical alteration in wingstroke kinematics as they compensated for the induced aerodynamic forces. This change included a dramatic increase in the upstroke velocity of the clipped wing, in a manner similar to that observed by Sugiura and Dickinson in rigidly held flies performing fictive turning maneuvers (H. Sugiura and M. Dickinson, in preparation), and a related difference in the timing of the “ventral flip,” the transition from upstroke to downstroke, which is correlated with wingbeat amplitude (Dickinson et al., 1993) and thus, yaw torque (Götz, 1987). The two wings remained in phase, however, beginning both upstroke and downstroke simultaneously. Some of these effects may also have been passive, resulting from changes in wing mass and shape. Flies with the posterior of their wing clipped did not obviously alter their wingbeats, but the model and my observations (above) indicate that they must have been actively compensating in order to maintain a stable orientation. Many changes in aerodynamic forces arise from subtle modification of wingstroke parameters that may not be obvious from such a superficial analysis, however (Götz, 1987; Lehmann and Dickinson, 1997; Fry et al., 2003). The anterior edge of the wing

includes many mechanoreceptors (Cole and Palka, 1982; Dickinson, 1990), feedback from which would be disrupted in the distal-clipped preparation but not in the posterior-clipped flies; this could also explain some of the differences seen in flight between the two types of preparation.

The ability of flies with clipped wings to stabilize their heading is partially dependent on vision. Figure II-7 shows characteristic traces from the flight of an intact fly and a posterior-clipped fly in a situation alternating between total darkness and a statically lit display. The average velocity and variability of the orientation of flies in darkness is much larger than in lit conditions, whereas these measures differ only slightly between intact flies and flies with clipped wings.

Another interesting component of flight on the magnetic tether is the presence of small oscillations in orientation, with a frequency of approximately 0.5 Hz (see Figure III-2). The functional significance of these oscillations is unclear, but they have also been noted in the ongoing wingbeat dynamics in rigidly tethered flies (M. Frye, personal communication). Although to my knowledge there are no published reports of such oscillations, they are particularly intriguing in view of the hypothesis that intersaccadic flight is straight in order to stabilize the visual image on the retina. If these turns are small enough not to cause image blur by rotating faster than a photoreceptor's acceptance angle per integration time constant, they may not cause significant degradation. It is conceivable that they could be homologous to microsaccades, one function of which is thought to be correcting for slow gaze drift (reviewed by Martinez-Conde

et al., 2004). An alternate, equally speculative explanation is that these oscillations are caused by sensory feedback delay during visual fixation, as discussed in Chapter I.

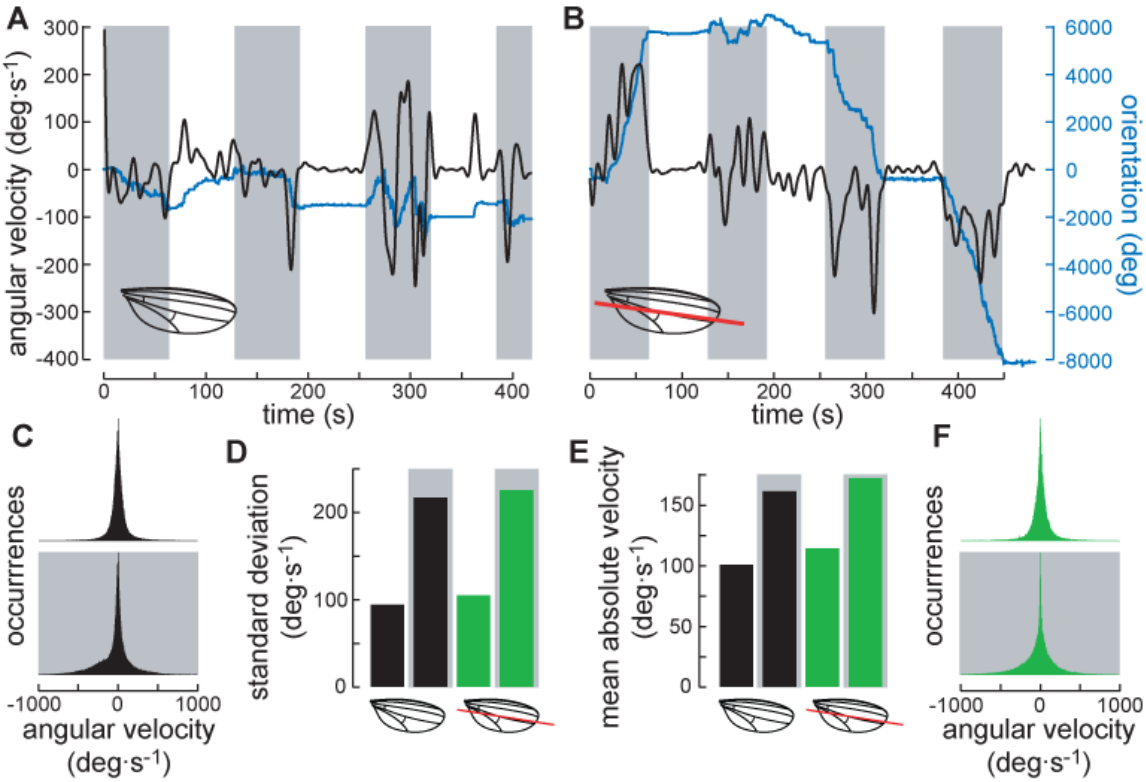

Figure II-7: Visual feedback is required for stability in both wing-clipped and intact flies. For these experiments, the arena lights alternated between 1 min on (data with white backgrounds) and 1 min off (gray backgrounds). Entire flight bouts are shown for **(A)** an intact fly and **(B)** a posterior-clipped fly. Black: angular velocity, lowpass-filtered at 0.1 Hz; blue: orientation. **(C,F)** Histograms of angular velocity for all flies tested in each condition (C: N=7 intact flies; F: N=3 clipped flies). **(D)** Standard deviations of the distributions in panels C and F. **(E)** The mean absolute value of all the velocity measurements taken in each condition (n=157024 intact-light samples; n=175648 intact-dark; n=59532 clipped-light; n=63265 clipped-dark).

III. Saccade Initiation

Recently, Tammero and Dickinson presented evidence that saccades in free flight are triggered by full-field visual expansion, and that rigidly tethered flies attempt to turn away from expanding square stimuli (Tammero and Dickinson, 2002a; 2002b). However, being unwilling to claim that the behaviors observed in rigidly tethered flies were truly saccades, they analyzed only average responses rather than the dynamics of individual saccadic events. With the magnetic tether, saccades are more easily discernible from non-saccadic flight, so I began a parameterization of the saccade response to visual expansion, although the existence of spontaneous saccades and other evidence indicates that saccades may be triggered through multiple pathways (Frye et al., 2003; Frye and Dickinson, 2004a).

Chapter Contents

Expansion Stimuli

I quantified the fly's collision-avoidance responses by challenging it with several types of stimuli designed to simulate the approach of a looming object. The time course of the angle subtended at the eye by such an object can be fully described by the ratio of two parameters: the object's half-length, l, and its velocity, v (Figure III-1A). For these experiments, I stimulated the fly with the projection on the arena of a virtual, square object with an edge half-length of 10 cm and one of several velocity profiles. I compared the responses of flies to objects approaching with constant velocities of 1.0, 1.5, or 2.0 $m \cdot s^{-1}$ and accelerating or decelerating objects, each somewhat faster than the fly's average cruising velocity of 0.3- 0.5 $m \cdot s^{-1}$ (David, 1978). The accelerating square had an initial velocity of 0 and accelerated at 6.2 $m \cdot s^{-2}$, and the decelerating square began at 3.4 $m \cdot s^{-1}$ and accelerated at −5.3 $m \cdot s^{-2}$ toward the fly. These parameters

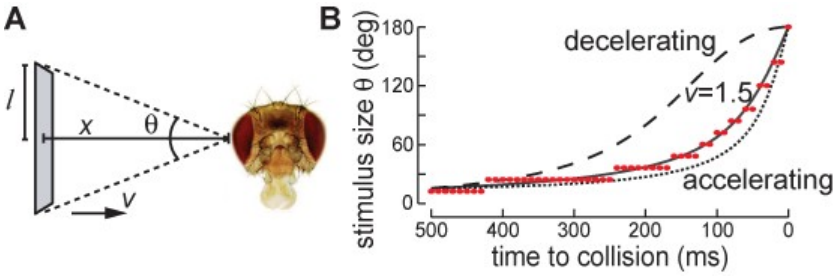

Figure III-1: Stimulus geometry and expansion profile. **(A)** The parameters l, an object's half-length, and v, its approach velocity, determine the angle subtended by the stimulus at the eye, θ, as a function of time. **(B)** The time course of stimulus expansion for the accelerating (dotted line), decelerating (dashed line), and one constant-velocity stimulus example (solid line; v=1.5 $m \cdot s^{-1}$). The red dots indicate the spatial discretization of the constant-velocity stimulus due to the diameter of the LEDs, sampled at 101 Hz (10 ms). *Drosophila* head photo courtesy of Prof. W. Gehring (biozentrum.unibas.ch/gehring; used with permission).

were matched to provide the same duration of apparent expansion as the object with a velocity of 1.5 $m \cdot s^{-1}$ (Figure III-1B). I also utilized a stimulus identical to the medium-velocity expanding object (v=1.5 $m \cdot s^{-1}$) but added alternating dark and light concentric stripes, maintaining a constant spatial frequency of 22.5° across the pattern. This stimulus was designed to increase the total visual motion in the pattern, enhancing the stimulation of Reichardt-type (delay-and-correlate) elementary motion detectors (EMDs) (Hassenstein and Reichardt, 1956; Reichardt, 1961) that may be used in fly motion vision (Egelhaaf et al., 1989; Borst, 1990). A third type of stimuli were formed by taking the medium-velocity expanding square and virtually masking it with either a horizontal, vertical, or diagonal slit. These masks ensured that each of the three stimulus types always had the same visual surface area on the arena, but contained motion along only one axis. The stimuli were temporally discretized by the pattern update rate and spatially discretized due to the LED displays, and so only provided a coarse simulation of real expanding objects. However, my results indicate that the flies discriminated behaviorally between the different stimuli (below), and in locusts, neural responses to expanding stimuli have been shown to be independent of the video refresh rate down to at least 67 Hz (Gabbiani et al., 1999).

Each trial consisted of a 10-s block which began with the presentation of a dark 22.5° square on a light background at a constant position within the arena. After the stimulus reached a size equivalent to 180° of azimuth, it remained at full size for about 5 s. In some trials, it immediately returned to its original state, whereas in others, it shrank back to its starting size with the inverse time course

to that with which it expanded. The order of the stimulus presentations was determined randomly, *ad hoc*, with the restriction that two successive stimuli be of different types.

Saccade Discrimination and Quantification

Offline, I analyzed the records of the fly's orientation in the magnetic tether arena using custom software written in Matlab (Mathworks, mathworks.com). Spontaneous behavior in this arena revealed periods of steady orientation interspersed with rapid changes in direction, or saccades (Figure III-2A; Movie III-1). I calculated each fly's angular velocity by applying an eighth-order, zero-delay, Butterworth filter to the orientation data, lowpass at one-fourth of the sample rate, and applying the central difference formula to the result, scaled using the timestamps saved for each frame. A histogram of these angular

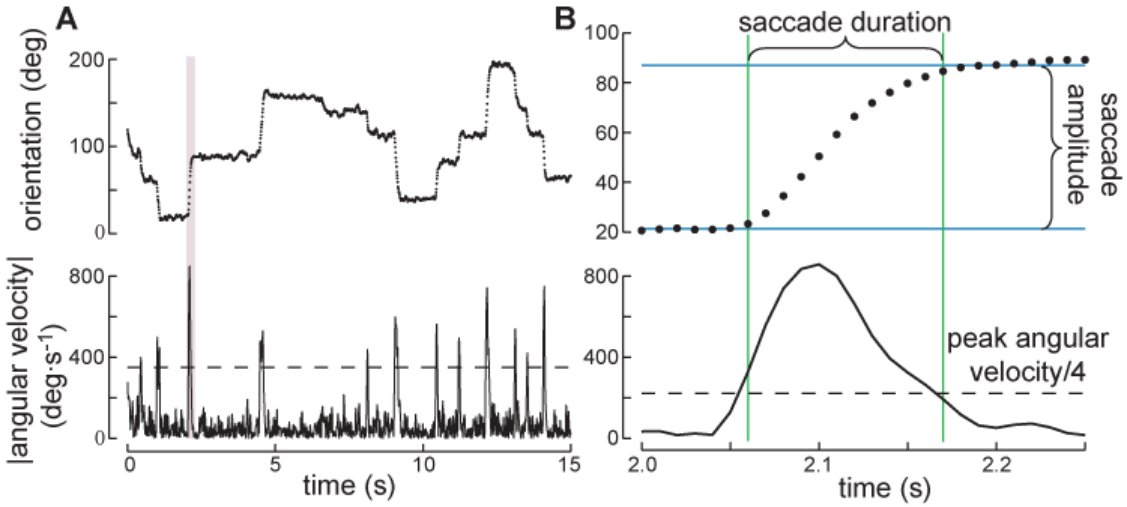

Figure III-2: Spontaneous saccades and saccade metrics. **(A)** Recorded orientation data (top), sampled at 101 Hz, and the fly's absolute angular velocity (bottom), estimated from the time course of its orientation. A velocity threshold was set at 350°·s^{-1} (dashed line) to separate saccades from non-saccadic flight. **(B)** Data defining one saccade, taken from the shaded region in panel A. Saccade duration (green lines) was the time during which the angular velocity exceeded one-quarter of its maximum value for that saccade (dashed line), and saccade amplitude (blue lines) was the difference between the median orientations during the 50 ms before and after the saccade.

velocities reveals a distribution similar to the sum of a Gaussian and an exponential distribution (Figure III-3), as reported by Mayer and co-workers (1988). The mean of the Gaussian was 0.31°·s^{-1} with a standard deviation of 87.7°·s^{-1}, and the exponential had a decay constant of 0.0017°·s^{-1}. This suggests an underlying system which has two states: a noisy, straight-flight state and an active, saccade state.

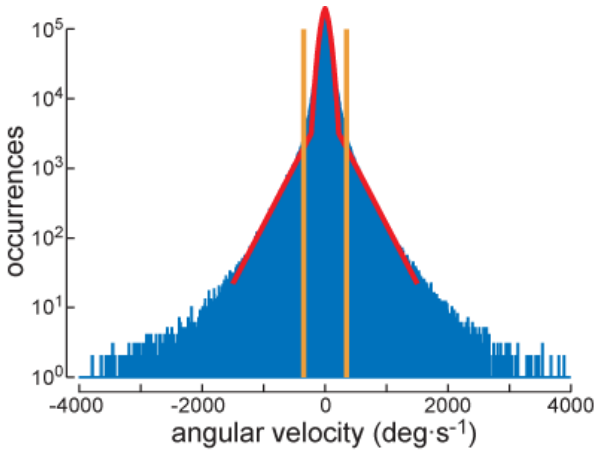

Figure III-3: Distribution of angular velocities observed during saccade stimulation in magnetically tethered flies (N=35 flies). The red trace is the sum of the Gaussian and exponential distributions fit to velocities below 1500°·s^{-1}(n=6,484,393 observations). The orange lines are at 0°·s^{-1}±4 s.d. of the Gaussian.

I separated saccadic events from straight flight by setting an angular velocity threshold at 4 s.d. away from 0°·s^{-1} (i.e., at ±350.8°·s^{-1}). I then quantified each saccade by determining its duration as the period during which the fly's angular velocity exceeded one-quarter of its maximum for that event (Figure III-2B). The amplitude of a saccade was then the difference between the fly's median orientations during the 50 ms immediately before and after the saccade. Only saccades with amplitudes between 15° and 150° were included for further analysis because of the increased likelihood that events with sizes outside that range represent tracking errors.

To measure the time of saccade occurrence relative to an expanding visual stimulus, I took data only from saccades initiated within a window of 500 ms, beginning 30 ms after the first discrete change in stimulus size. During the trials

in which the object approached at 1.0 $m \cdot s^{-1}$, however, this period did not include the time of the virtual collision. Therefore, I analyzed a 500-ms window starting 280 ms after the beginning of the stimulus. Examination of the distribution of saccade initiation times over the entire course of stimulus expansion suggested that the saccadic frequency was no different during the initial 250 ms than in an equal length of unstimulated time (data not shown). If two or more saccades occurred within the 500-ms analysis window, only the first was included. I compared the probability of saccade initiation during this window with that calculated during a similar window located 3 s after a stimulus presentation (Figure III-4A).

Evocation of Saccades by Expansion

I presented magnetically tethered flies with visual stimuli designed to simulate a looming, square object with various approach velocities, shapes, or textures (Figure III-4). During presentations of these expanding stimuli, flies showed a significantly increased frequency of saccades than during a similar period without expansion (ANOVA, $p<0.01$ for all stimulus types). However, the probabilities of response to different types of expanding stimuli were statistically indistinguishable ($p>0.05$). In addition, because some studies have suggested ambiguity about whether flies avoid visual expansion or fixate contraction (Tammero et al., 2004), I estimated the saccade probability during the contraction of identical visual stimuli. This analysis indicated a significantly decreased

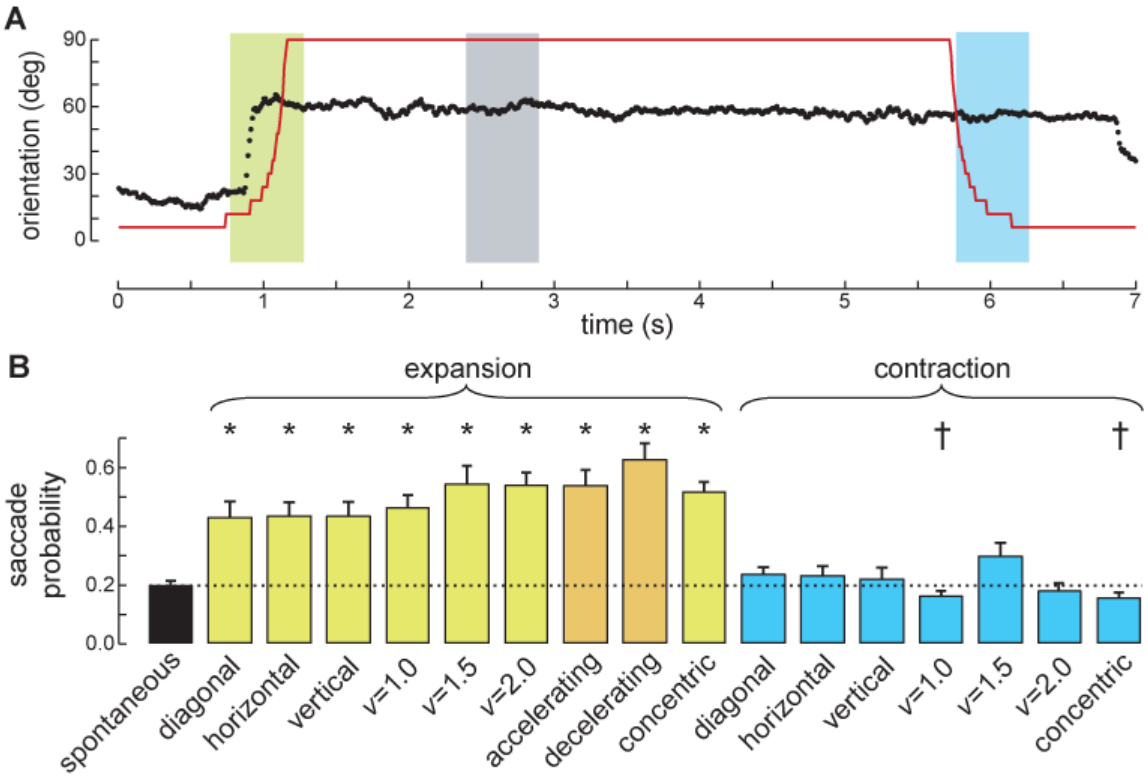

Figure III-4: Stimulus expansion triggers saccades. **(A)** The half-size of the stimulus (red trace) overlaid with the fly's orientation (black dots), sampled at 101 Hz during a single expansion trial. Saccades initiated within a 500-ms window during stimulus expansion (green box) were labeled as visually elicited. Likewise, saccades were tabluated which occurred during stimulus contraction (blue box) or during a similar window with no stimulation ("spontaneous"; gray box). **(B)** There was a significantly higher probability of observing a saccade during stimulus expansion than during no stimulation (ANOVA, *: $p<0.01$), and the saccade rate was independent of expansion parameters (ANOVA with Bonferroni correction for multiple comparisons, $p>0.05$). Contraction of a slowly moving or concentrically striped stimulus inhibited saccade generation (†: $p<0.05$). N=35 flies; n=2933 saccades, although not all flies received all stimulation conditions.

saccade frequency during visual contraction for only two of these stimuli ($p<0.05$) – the stimulus with the slowest approach velocity and the concentrically striped stimulus.

Another finding of Tammero and Dickinson was that the avoidance response to visual expansion in rigidly tethered flies showed an increased latency to stimuli presented frontally, compared to stimuli presented somewhat to one side (Tammero and Dickinson, 2002b). This coincided with an increased

probability of a landing response, in which flies extended their forelegs (Goodman, 1960; Wagner, 1986; Borst, 1986). They argued that the two reactions operate *via* independent neural pathways, but that the decrement in the turning response provided an increased probability for the fly to successfully land. From my data on visually elicited saccades, in which the fly was free to rotate relative to the fixed stimulus location, I extracted the probability of saccade initiation as a function of the fly's heading relative to the position of the stimulus at the beginning of expansion (Figure III-5). I found the same trend as that observed by Tammero and Dickinson (2002b), in which stimuli located near ±90° had a higher probability of eliciting a saccade than stimuli presented frontally. This probability drops again as the stimulus position approaches the rear of the animal, but even expansion located near 180° had a slightly higher chance of eliciting a saccade than the spontaneous rate. Expansion of a visual object therefore has a significant likelihood of evoking a saccade, and this probability is dependent on the orientation of the fly relative to the object. Some of the deviations that I observed from this trend are likely due to the fly-to-fly differences in the relative alignment of the camera and flight arena, estimated at ±5°.

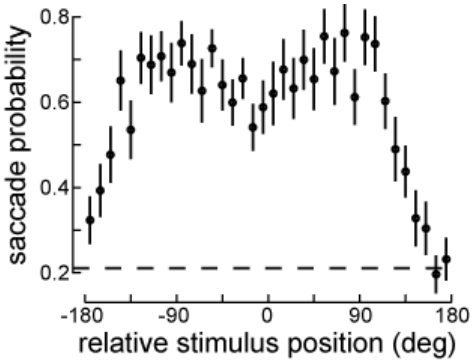

Figure III-5: Response probability varies with expanding stimulus position, with the highest probability observed to stimuli located to either side of center. Values are mean±s.e.m. Dashed line indicates the spontaneous saccade rate.

Saccade Timing and Visual Stimulation

Modeling of saccade initiation

The above analysis ignores saccade timing relative to the expansion stimulus as a potential cue to the neural processes underlying visually elicited saccades. Tammero and Dickinson (2002b) reported that the latency of the turning response was nearly constant relative to the onset of visual expansion, becoming slightly longer for very slow expansion, but they do not report how they calculated this latency. In addition, their square stimuli expanded with a constant angular velocity, whereas mine took into account the geometry of a looming object. Figure III-6 shows a peristimulus time histogram (PSTH) of normalized saccade probability in the time window during which saccades were considered to be visually elicited. This shows that virtual objects with a faster velocity tended to evoke saccades later, in a clear conflict with a time-to-contact response model. The seeming appearance

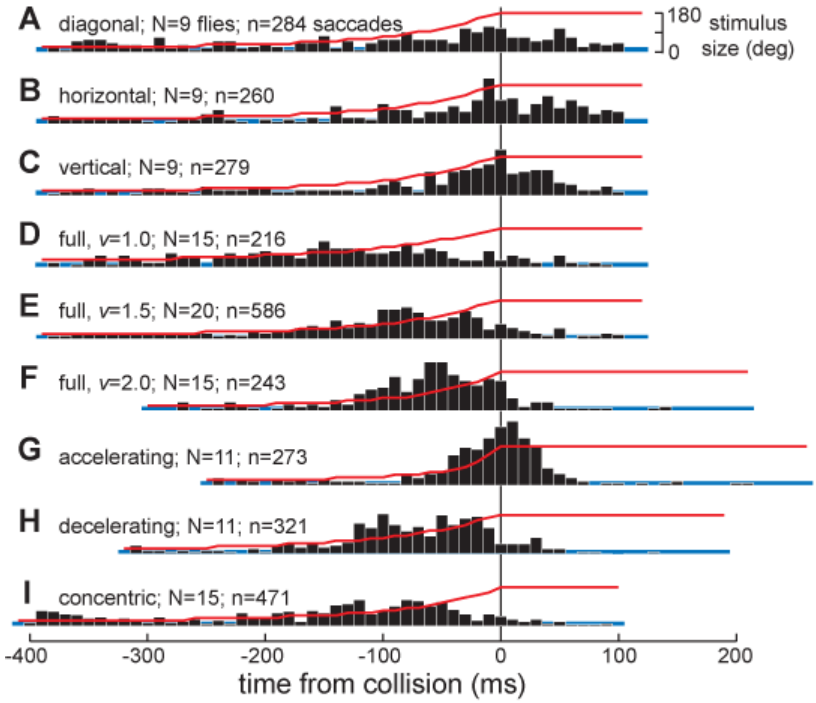

Figure III-6: The time course of saccade probability is dependent on the time course of stimulus expansion. **(A-I)** Peristimulus time histograms (black) of the relative probability of saccade initiation during the 500-ms window qualifying saccades as visually elicited, beginning 30 ms after the first discrete change in stimulus size for each type. Red traces show the stimulus angle, and blue shading indicates the spontaneous saccade rate. Data were collected at 101 Hz, and are therefore binned at 10 ms.

of a refractory period after the time of virtual collision could be an artifact of the data analysis: if more than one saccade occurred within a single stimulus presentation, only the first was counted, although saccades were only observed in about 50% of the trials (see Figure III-1).

To develop a neurally based hypothesis explaining the initiation of saccades in response to expanding stimuli, I utilized the theoretical framework developed by Gabbiani and co-workers to describe the responses of the locust descending contralateral motion detector (DCMD) neuron to presentations of similar, looming stimuli (Hatsopoulos et al., 1995; Gabbiani et al., 1999; 2001). Regardless of whether the stimulus represented an expanding circle or square, they found that the DCMD neuron's peak spike rate occurred with a fixed delay after the object reached a critical angular size. This critical size was independent of the time course of visual expansion, fitting tightly to the equation:

$$t_{peak} = \alpha \frac{l}{v} - \delta \ , \qquad \text{(III-1)}$$

where t_{peak} is the time of the peak neural firing rate, l and v are, respectively, the half-size and velocity of the virtually expanding object, and $-\delta$ represents the delay term. From the coefficient α, one can calculate the critical stimulus size, θ_{crit}, as:

$$\theta_{crit} = 2 \tan^{-1} \frac{1}{\alpha} \ . \qquad \text{(III-2)}$$

Because the relationship between t_{peak} and l/v is linear, θ_{crit} must be a constant.

Saccade timing and the angular threshold model

I used this model to see if the probability of saccade initiation followed the same relationship, with the implicit hypothesis that a homolog, or a homologous neural circuit, exists in the fruit fly. I used the probability of saccade initiation as a behavioral proxy for the activity of a hypothetical homolog in the fly to the locust DCMD neuron, and estimated its parameters using the equations above. Although the constant-velocity expanding stimuli only represent three values of l/v, I utilized the accelerating and decelerating stimuli to provide better constraints for the model. First, I filtered the function describing the time course of saccade probability for each stimulus using a 5 Hz lowpass, zero-delay, Butterworth filter, and extracted t_{peak} as the time of this function's peak value. For the accelerating and decelerating stimulus, l/v is a function of time, so I began by taking its value at $t=t_{peak}$. A least-squares, linear, best fit to these values of t_{peak} and l/v provided an initial estimate for α and δ, where $t=t_{peak}-\delta$ represents the time at which the stimulus reached critical size. I replaced l/v in the regression equations with its value at $t=t_{peak}-\delta$ and refit the model, iterating this procedure until α and δ converged to constant values, i.e., when δ had changed by less than 0.01 ms since the previous iteration. Convergence was generally achieved within 5-10 iterations.

I filtered the PSTH function and took the time of its peak value, and plotted this as a function of the inverse of the stimulus velocity (Figure III-7). A best-fit line to the data derived from the full-sized, uniformly textured, expanding square stimuli had a regression coefficient (r^2) of 0.91, indicating strong evidence for a linear fit and therefore a critical angular size for the stimulus. From this line and Equation III-2, the critical angle (θ_{crit}) was 62°, and the delay (δ) between the time the stimulus reached this threshold size and the time of the peak saccade probability was 49 ms. For comparison, taking only data from the constant-velocity squares yielded an r^2 value of 1.00, with θ_{crit}=71° and δ=22 ms. Both values are on the order of those reported by Gabbiani et al. of θ_{crit}=15-40° and δ=5-40 ms, varying across individuals (Gabbiani et al., 1999; 2001), and the 20- to 30-ms delay observed in the chasing response of the housefly (Land and Collett, 1974; Collett and Land, 1975). The time of peak saccade probability for

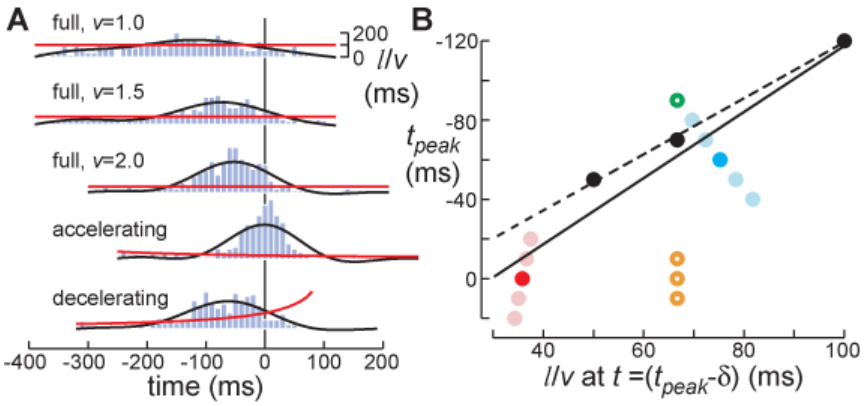

Figure III-7: Saccade initiation probability peaks at a constant critical stimulus size. **(A)** The time of peak saccade probability (t_{peak}) for each stimulus type was extracted from the PSTHs of Figure III-6 by application of a 5-Hz lowpass filter (black traces). The values of l/v as a function of time (the stimulus half-size divided by its velocity (see Figure III-1); here, this is equivalent to $1/v$) are shown as red traces over each histogram. **(B)** The relationship of l/v to the time of peak saccade initiation probability is linear when corrected for the changes in l/v occurring between stimulation and response. The filled, black circles indicate the response times to the full, constant-velocity stimuli. The filled, red and blue circles show t_{peak} for the accelerating and decelerating stimuli, respectively. The red and blue shadows demonstrate how the location of these points would vary with different values of t_{peak}; the other points would shift only vertically, as l/v is constant. The solid, black line is a least-squares fit to the filled circles; the dashed, black line is fit to the filled, black circles only. The open, orange circles indicate the responses to the partial (horizontal, vertical, and diagonal) motion stimuli; the open, green circle is the response to the concentrically striped stimulus.

the partial (masked) stimuli is much later than that for the equivalent full square, and the peak time for the concentrically striped square stimulus is slightly earlier; the implications of this will be discussed later (Chapter VI).

Quantifying Saccade Dynamics

Metrics of saccade dynamics

After separating saccadic events from non-saccadic flight in magnetically tethered flies, I made use of three saccade metrics: absolute amplitude (the angular size of the turn), duration, and peak absolute angular velocity. Figure III-8 shows the logarithmic distributions of these parameters. The average amplitude of a saccade (mean±s.d. of a log-normal fit to the histogram) was 35.2±1.6°; the duration was 78.5±1.4 ms; and peak velocity was 637.8±1.4°·s^{-1}. Two-dimensional histograms show the relationships between these metrics (Figure III-9). It is intuitive, but was not certain *a priori*, that saccade amplitude and peak velocity should be tightly related; the Pearson coefficient of correlation (ρ) for these two metrics is 0.70. Amplitude and duration also covary, with ρ=0.59, but some additional spread is apparent for larger saccades. However, duration and peak angular velocity are not coupled, as ρ=0.06 (not shown). This suggests, speculatively, that rather than controlling each metric separately, only saccade amplitude may be under active control, with duration and peak velocity partially dependent upon amplitude. These correlations are evocative of the so-called

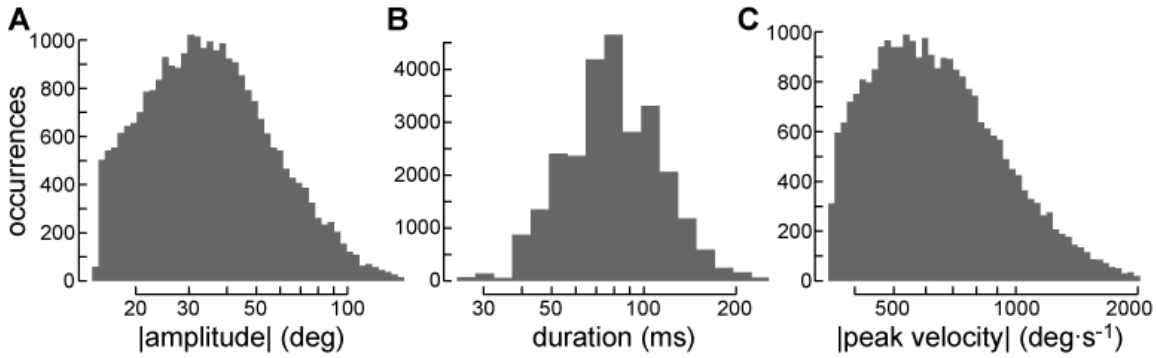

Figure III-8: (A-C) Saccade absolute amplitudes (A), durations (B), and peak absolute angular velocities (C) are log-normally distributed. N=35 flies; n=26535 saccades. The histograms are truncated: only saccades with amplitudes between 15° and 150° were analyzed, and events with peak angular velocities below 350°·s^{-1} were not classified as saccades.

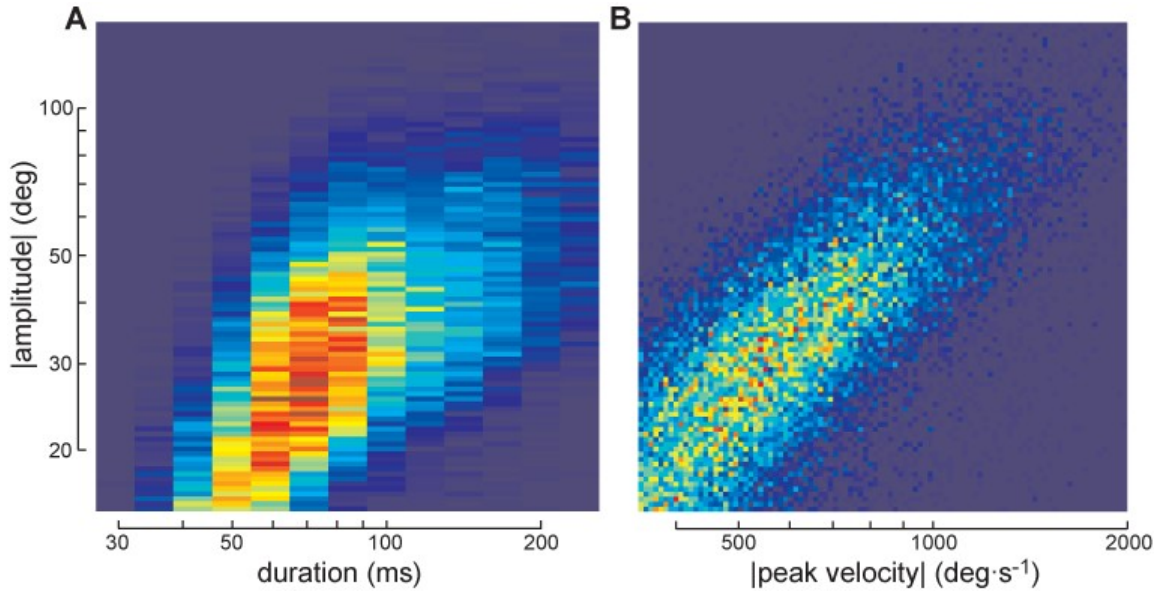

Figure III-9: Two-dimensional histograms **(A,B)** show that saccade amplitude is correlated with duration and peak angular velocity. Saccades with amplitudes <15° were not analyzed due to the difficulty discriminating them from non-saccadic flight.

"main sequence" relationship between the amplitude, duration, and peak velocity of saccades in humans and other primates (Bahill et al., 1975; Ramat et al., 2007).

Predicting saccade dynamics

In order to quantify how well saccade dynamics (amplitude, duration, and peak angular velocity) could be predicted by properties of the stimulus, I used *k*-

fold cross-validation, a jackknife statistical technique, with *k*=10. This process required randomly splitting the data into 10 (*k*) blocks and using 9 of those blocks to build a model predicting the values in the last block. I took the mean-squared error (MSE) of the prediction as the measure of performance, averaged across 10 iterations such that each block was used exactly once for testing. I used a second-order polynomial model, and compared the MSE of the prediction to the naïve MSE (i.e., the overall variance of each saccade metric) to describe how much of the variation in behavior could be explained by various parameters of the stimulus. The orientation of the stimulus relative to the fly had a modest (10–12%) predictive value for saccade amplitude and peak velocity and could account for some of the skew in the histograms of these metrics (Figure III-8), but none of the other tested stimulus parameters were related to any of these measures of saccade dynamics (Figure III-10). A first-order polynomial model had slightly less predictive power than the quadratic form, but increasing the polynomial order beyond two did not improve the predictions; nor did an exponential model perform any better (data not shown). The flies consistently fixated one orientation in the magnetic tether arena more than the others (Figure III-10A, bottom), which was not centered on the stimulus even when the slight uncertainty about the relative orientations of the fly and the visual arena was accounted for. This may correspond to one vertical edge of the square stimulus or result from a slight misalignment of the magnets, but no asymmetries in saccades were observed (Figure V-6, Figure V-10).

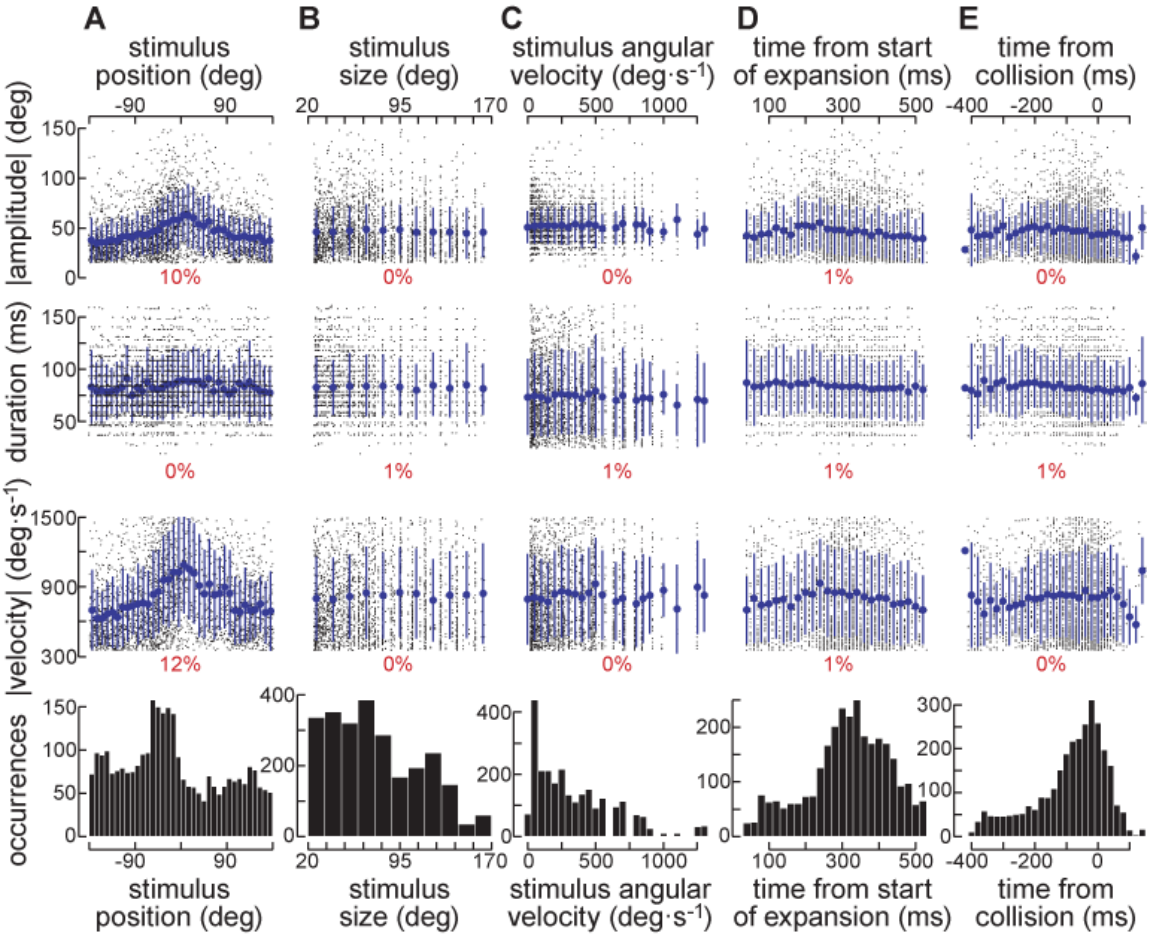

Figure III-10: Some of the variation in saccade metrics (rows: amplitude, duration, peak angular velocity) can be predicted from stimulus parameters (columns **A-E**). The red numbers quantify the reduction in uncertainty about a saccade metric given the value of the corresponding parameter at the time of saccade initiation. Blue traces indicate the mean±s.d. in each bin; black dots illustrate the results from individual stimulation trials. N=35 flies; n=2933 saccades.

IV. Active Modulation of Halteres

The halteres normally act to restore flight equilibrium in the presence of perturbations (Dickinson, 1999; Sherman and Dickinson, 2003). This raises the question of their role in active flight maneuvers, as a naïve observer might expect that they would quickly cancel out any attempted turn. One way that nervous systems avoid such conflicts is by sending an efferent signal to a sensory system that is opposite in sign to the expected, reafferent input from a motor plan. This is called an efference copy or corollary discharge (von Holst and Mittelstaedt, 1950; Sperry, 1950; for a recent review, see Poulet and Hedwig, 2007). An efference copy sent to the halteres might be mediated by the haltere steering muscles, serial homologs of the wing steering muscles (Bonhag, 1949; Mickoleit, 1962). Chan and co-workers found that visual input can drive action potentials in these muscles, supporting this possibility, but the functional consequences of this activity are unclear (Chan et al., 1998).

A slightly modified version of this hypothesis would be one in which the haltere steering muscles are activated before, and possibly instead of, direct, descending commands to the wing steering muscles (proposed by Chan et al., 1998). In this scheme, the haltere steering muscles would act to deflect the haltere out of its stroke plane, simulating an angular rotation of the fly's body. The haltere's mechanosensors would initiate their normal response to this fictive rotation, leading to changes in wingstroke kinematics (Chan and Dickinson, 1996; Fayyazuddin and Dickinson, 1996; 1999) that cause a turn. Therefore, instead of using descending activation of the haltere steering muscles to cancel the

forthcoming, reafferent haltere input, contraction of these muscles might begin a sequence of events which causes a turn. Both of these hypotheses depend on active modulation of the halteres, and observing this is practically impossible in magnetically tethered flies. Therefore, I utilized a rigidly tethered preparation to determine whether the haltere strokes are modulated during flight, and if so, whether this modulation precedes changes in the wingstrokes.

Chapter Contents

Rigidly Tethered Flies

A subset of flies were prepared for “rigidly tethered” experiments (after Kunze, 1961; Fermi and Reichardt, 1963), in which a tungsten wire (either 0.1 or 0.25 mm in diameter) replaced the steel pin used to magnetically tether flies. In these flies, I attached the wire perpendicular to the body axis, placing it such that the fly's head was fixed relative to the thorax. The wire was held during experiments such that the body angle was fixed at around 45°. I used two, similar visual arenas for rigidly tethered flies. Both were cylinders formed of LEDs; one

consisted of 4x9 LED panels, each identical to the panels used for the magnetic tether arena, encompassing in total 270° of azimuth with 32x72 LEDs, yielding an average azimuthal subtense of 3.8° for each LED. The second arena was designed to perform high-resolution stimulation, spanning 316° of azimuth using 63x180 LEDs for an average of 1.8° of azimuth per LED (Sherman and Dickinson, 2003). In both cases, the fly was illuminated in the near-infrared spectrum by a single LED positioned overhead. A pair of photodiodes aligned beneath the fly measured the shadow cast by the two wings (Figure IV-1). One major way in which flies produce aerodynamic forces is by differentially modulating the downstroke amplitude of the wings: a large difference in wingbeat amplitude (abbreviated as L−R WBA) corresponds to a yaw turn, and the sum of the amplitudes (L+R WBA) correlates with the fly's attempts to produce pitch torque (Vogel, 1967; Götz, 1987; Dickinson and Lighton, 1995; Lehmann and Dickinson, 1997; 1998). These signals were monitored on a stroke-by-stroke basis by a “wingbeat analyzer” (Götz, 1987; Dickinson et al., 1993) and used to control the azimuthal angular velocity of a pattern in a closed-loop manner. Before comparative analysis, I normalized the left and right WBA signals from each fly to have a standard deviation of 1, in order to correct for slight differences in each fly's positioning relative to the photodiodes (Tammero and Dickinson, 2002b).

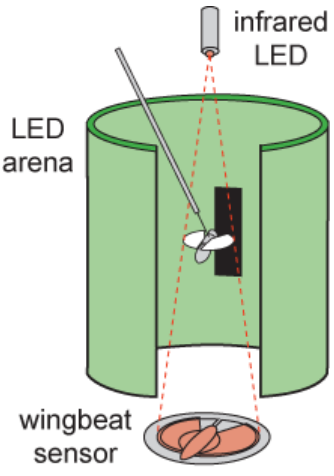

Figure IV-1: Rigid tether arena and closed-loop behavioral monitoring system.

For preparations involving alterations of the halteres, I made the manipulations to cold-anesthetized flies before tethering them to the pin. In one group of experiments, I applied a small amount of UV-activated cement to the endknobs of both halteres, approximately doubling the volume of the endknobs. For another set of flies, I ablated the left haltere by pulling gently on the endknob with a pair of fine forceps until the stalk detached from the base (after Dickinson, 1999). This technique generally left the df2 campaniform sensillum intact, which is thought to be responsible for sensing deflections of the haltere from its stroke plane (Pringle, 1948; Fayyazuddin and Dickinson, 1996; Dickinson, 1999; nomenclature from Gnatzy et al., 1987). In general, unrestrained flies with halteres either weighted or ablated were capable of stable flight, consistent with Fraenkel's observations (1939) and indicating that the alterations were not so drastic as to cause catastrophic failure of the fly's flight control system.

Saccades in Rigidly Tethered Flies

Saccade identification and visual stimulation

To extract saccades from non-saccadic flight in rigidly tethered flies, I used a slightly different method than in magnetically tethered flies because the relationship of the recorded torque signal (L−R WBA) to the fly's angular velocity on the magnetic tether is not clear. I extracted the mean values of the fly's L−R WBA during a few 200-ms windows spanning a total range of 500 ms. If any of these values exceeded the mean±2.5 s.d. of the L−R WBA during the 1 s before a trial began, the event was classified as a saccade. Saccade duration was

defined as the time surrounding the peak in the L−R WBA signal during which the filtered derivative of L−R WBA (estimated by the central difference method) did not change sign. Saccade amplitude depends on the gain of the experimental coupling between pattern position between L−R WBA, and was not analyzed.

To visually elicit saccades in rigidly tethered flies, I used the same expansion profile as the 10-cm square approaching at 1.5 $m \cdot s^{-1}$ that I used in magnetic-tether experiments, except that the object began with a height:width ratio of 2:1 (a short, vertical stripe) because recent results by Maimon and Dickinson indicate that both freely flying and rigidly tethered flies avoid squares but fixate objects with an aspect ratio of 2:1 or higher, actively maintaining them in a generally frontal position (Maimon and Dickinson, 2006). The stimulus morphed into a square by expanding twice as quickly in the azimuthal plane as in the elevational, and then remained at full size for 1 s, after which it immediately reverted to the initial stimulus. Between trials (5, 10, or 15 s), the azimuthal position of the stripe was controlled in closed loop by the fly's L−R WBA. For flies in which I was visualizing the halteres, the stimulus was always a full-height stripe (aspect ratio 8:1), and when it expanded, it did so only horizontally.

During haltere visualization, in addition to the visual evocation of saccades, I stimulated a separate group of flies with patterns of visual motion simulating pure rotation about the yaw, pitch, or roll axes. The yaw rotation stimulus consisted simply of vertical stripes with a spatial frequency of 22.5°, and the stimuli for pitch and roll were identical patterns of roughly spherical motion

shifted by 90° of azimuth relative to each other (see Figure IV-8, top row). These stimuli were separated by 10 s of closed-loop control over the position of a vertical stripe.

Saccade stimulation

After confirming that magnetically tethered flies performed saccades in response to visual expansion, I presented similar stimuli to rigidly tethered flies in order to study their behaviors and to investigate the possible effects of haltere manipulations. I used a stimulation paradigm comparable to the one I used for saccades in magnetically tethered flies and the one Tammero and Dickinson (2002b) used on rigidly tethered flies. A fly actively controlled the azimuthal position of a stimulus object in closed loop by modulating wingbeats, as recorded by the wingbeat analyzer circuitry. The difference between the left and right wingbeat amplitudes (L−R WBA) is proportional to the torque produced by the fly (Vogel, 1967; Götz et al., 1979; Lehmann and Dickinson, 1997). The stimulus was a vertical bar with a 2:1 aspect ratio, which expanded into a square at arbitrary times by growing twice as fast in the horizontal direction as in the vertical. Extracting saccades as events in which the variance of the L−R WBA signal

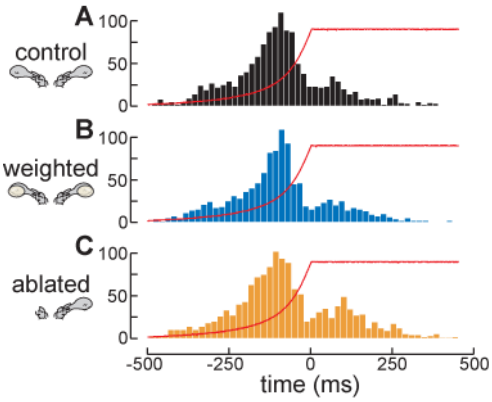

Figure IV-2: Peristimulus time histograms of saccade initiation by rigidly tethered flies responding to an expansion stimulus (red traces). **(A-C)** Haltere treatments (see text) did not affect the time course of saccade probability.

exceeded a threshold relative to a prestimulus interval, I found that expanding visual stimuli also have a high probability of eliciting saccades in rigidly tethered flies (Figure IV-2).

I made an additional test of whether saccade stimulation required a coherent stimulus object or could be elicited by large-field expansion. In these experiments, rigidly tethered flies were presented with a pole of expansion and a pole of contraction in a horizontal square wave pattern with a fundamental spatial frequency of 42°. This was similar to the calibration stimulus used for the magnetic tether arena, with the poles fixed at ±90°. If the fly produced a non-zero L−R WBA signal, the pattern shifted to produce visual expansion from the side the fly was steering toward. Flies were stimulated in this closed-loop fashion for 10 s, which strongly induced straight flight. At that time, the pattern shifted sideways at a temporal frequency of 2.9 Hz for a varying duration of time, and then was held static for 500 ms. I found that a shift of only 25 ms (2 pixels, or 3.6°) led to an average saccade probability of 0.2, while increasing this to 500 ms (35 pixels) led to a mean saccade probability of 0.33 (Figure IV-3). Neither of these was significantly different from the average spontaneous saccade rate calculated during the object-expansion trials (p>0.05).

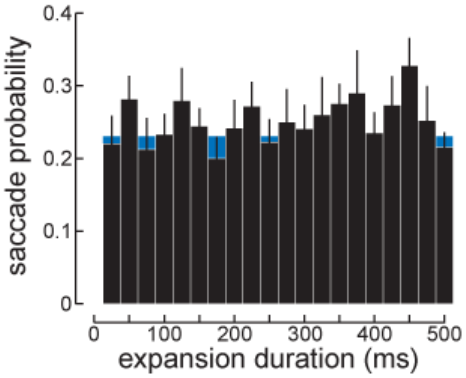

Figure IV-3: Saccade probability increases slightly with the duration of a full-field expansion stimulus centered at ±90°. Bars show mean±s.e.m; the blue shadow reflects the spontaneous saccade rate. N=28 flies, n=2782 trials.

Doubling the mass of the haltere endknobs with glue significantly increased the peak L−R WBA during a saccade (p<0.01) but not the duration, and ablating the left haltere had no effect (Figure IV-4). Overall, flies with their halteres weighted produced a larger L−R WBA signal and a larger L+R WBA signal during saccades than control flies (Figure IV-5). Flies in which one haltere had been ablated showed virtually no differences from intact flies in

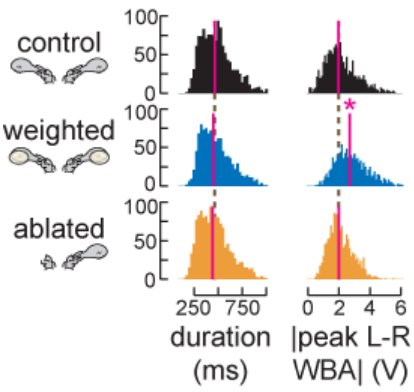

Figure IV-4: Weighting the halteres affects peak torque production (measured as the difference between left and right wingbeat amplitudes, L−R WBA) during saccades by rigidly tethered flies. Top row: N=9 intact flies, n=1542 saccades. Middle: halteres weighted with glue droplets (N=7, n=1300). Bottom: left haltere ablated (N=11, n=1390). (*: p<0.01; ANOVA with Bonferroni correction for multiple corrections). Pink bars show the median value of each histogram.

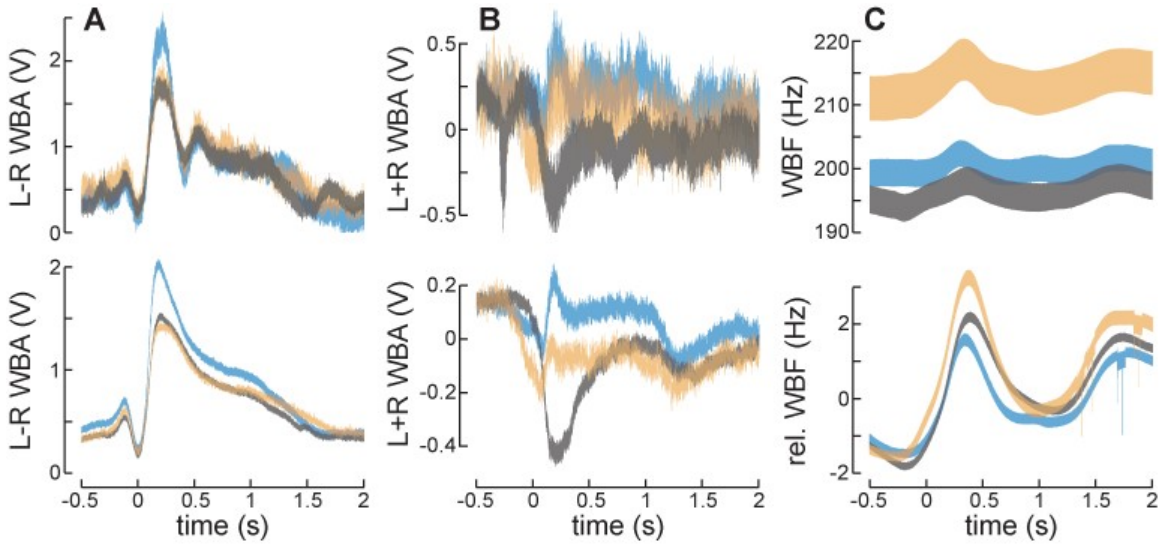

Figure IV-5: The time course of visually elicited saccades is altered in rigidly tethered flies when the halteres are weighted (black: control, N=9 flies; blue: halteres weighted, N=7; orange: left haltere ablated, N=11). In each panel, the top row includes only saccades with a measured duration between 400 and 425 ms (n=71 intact saccades; n=68 weighted; n=82 ablated), and the bottom row is the average of all saccades recorded (n=1316 intact; n=1122 weighted; n=1390 ablated). The envelopes show the mean±s.e.m. **(A)** In the L−R WBA signal, corresponding to the production of yaw torque, the peak value is increased in flies with weighted halteres. **(B)** Haltere manipulations have a slight effect on L+R WBA, which is related to pitch torque and total force. **(C)** Flies with one haltere ablated display an elevated wingbeat frequency (WBF). All traces are aligned to the time of saccade initiation (t=0), and centered vertically such that the mean value in each trial is 0 over the 2 s preceding the saccade. For the top plot in panel C, the wingbeat frequency is re-centered to its presaccadic mean.

average time course or dynamics (Figure IV-6), other than an elevated wingbeat frequency, as previously noted by Dickinson (1999). These data imply an active role for the halteres in saccade initiation because no rotation or Coriolis forces were experienced by these flies.

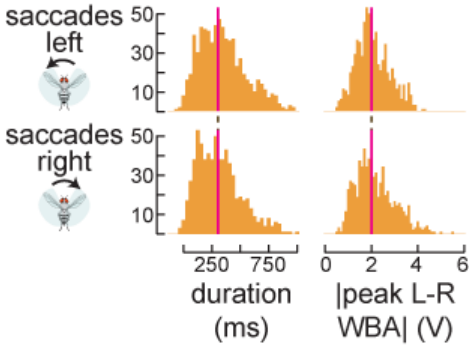

Figure IV-6: The dynamics of saccades to the right and to the left do not differ in rigidly tethered flies with the left haltere ablated (N=11 flies, n=706 saccades left, n=662 right; ANOVA, $p>0.05$).

Correlation of Wing and Haltere Strokes

Phase-locked video

The wingbeat analyzer used in the rigid tether arena outputs a synchronizing pulse near the end of each downstroke, which I used in one set of experiments to generate an *a priori* estimate of the next wingstroke period using a dedicated PC running a real-time Linux kernel module. By averaging the periods of the preceding 5 wingstrokes, I predicted the duration of the next stroke and output a voltage pulse at a constant phase relationship to the wingstrokes. This signal triggered an array of red LEDs and a camera to capture images of the fly, focused on the right haltere, illuminating the LEDs for 300 μs at a phase delay of 0.98 relative to the synchronizing pulse. For a fly with a wingbeat frequency of 200 Hz, this meant that the strobe and the image capture began 100 μs before the synchronizing pulse and ended before the wing's ventral flip (Dickinson et al., 1993). The variability of the phase relationship between the wingbeat and the images was dominated by the 50-kHz polling frequency (20-μs period) of the software, as the wingbeat frequency changes only gradually (see Figure IV-5).

These phase-locked videos were annotated by hand to extract the both the maximum and minimum stroke positions of the haltere in each frame. Although the precise alignment of the camera and the fly varied slightly for each fly, I estimated the stroke angle of the haltere by calculating the angle of inclination from the horizontal of a line defined by the average of the maximum and minimum haltere stroke points and a fixed point located near the edge of the image (Figure IV-7 and Movie IV-1). I added a small amount of cadmium yellow paint to the tip of the haltere to increase its contrast.

I used the haltere stroke angles derived from this video analysis to determine the strength and timing of the correlation between haltere stroke phase and wingstroke amplitude. This was calculated for a single trial by first normalizing the haltere angle and the wingbeat signal to a mean of 0 and a standard deviation of 1 and then temporally shifting the haltere data relative to the wingbeat data collected by the wingbeat analyzer. For each shift, I calculated the cross-correlation of the two signals in order to determine whether the maximum correlation was achieved simultaneously or with some delay.

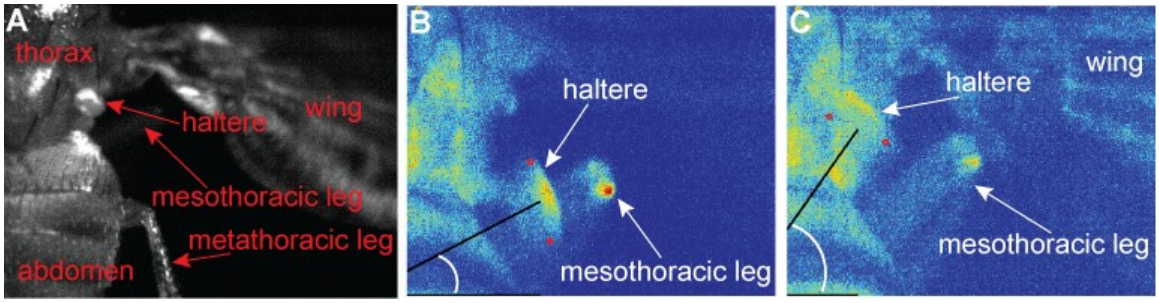

Figure IV-7: (A) Video image taken with additional lighting. **(B,C)** Pseudocolored, single frames of phase-locked video from a single trial (the same trial as in Figure IV-9). Note the widely divergent angle of the haltere between the two frames. The small, red circles on either side of the halteres were placed by hand to approximate the haltere's maximum and minimum stroke extent during a single frame (300-µs exposure). The angle described by the white arc is the haltere's stroke angle, defined by the black lines intersecting at (-50, 250), where (0, 0) is the top left corner of the image. The other end of the black lines is set by the average position of the two red circles.

Relationship between wing and haltere strokes

First, I presented the fly with pure rotational motion around one of the three primary axes (yaw, pitch, or roll) and monitored its wingbeat responses while simultaneously collecting phase-locked video, from which I manually extracted the stroke angle of the haltere relative to the body. Flies respond behaviorally to such stimuli with strong syndirectional turning (Götz, 1964; Götz et al., 1979; Blondeau and Heisenberg, 1982; Götz and Wandel, 1984), and the results of this experiment indicate that the phase relationship of the left wingbeat amplitude to the right haltere stroke is altered during fictive turns in one direction relative to the other direction, about all three axes (Figure IV-8). In addition, I collected phase-locked video while challenging flies with expanding visual stimuli (Figure IV-9).

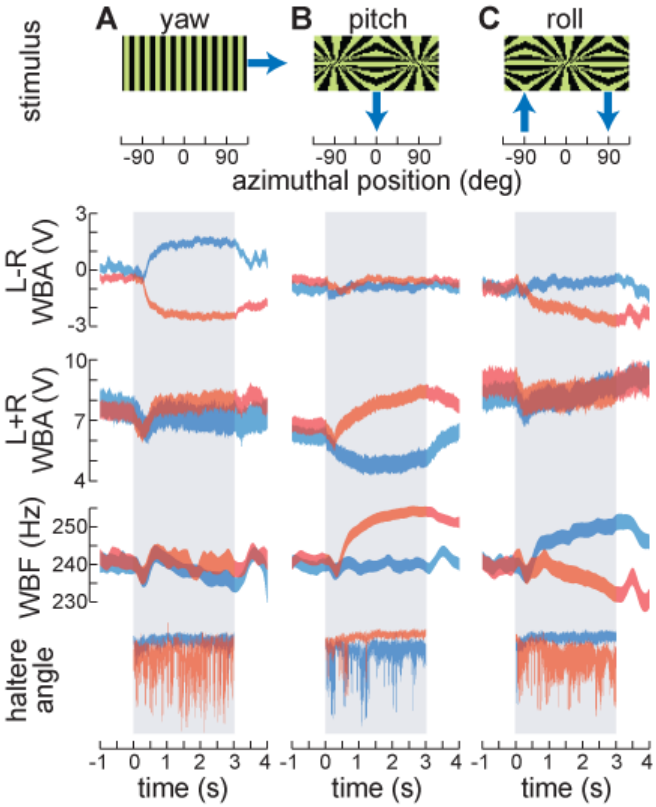

Figure IV-8: Haltere stroke angle alters its phase relationship with the left wing during active turns by rigidly tethered flies. Flies were stimulated with pure visual **(A)** yaw, **(B)** pitch, or **(C)** roll. The blue arrows by each stimulus indicate the direction the stripes moved during a positive turn, defined about each axis by the right-hand rule. Blue data traces correspond to the flies' responses to stimuli in the positive direction; red traces are responses to negative-direction stimuli. The gray boxes denote the visual stimulation period; outside of this time the fly was actively controlling the azimuthal position of a vertical stripe. Envelopes indicate the mean±s.e.m. N=5 flies. For yaw, n=32 trials in the positive direction; n=53 negative; for pitch, n_+=67, n_-=93; for roll, n_+=48, n_-=37. For haltere angle, one trial was digitized from each fly for each stimulus type in each direction (n=5) except for negative pitch, which includes an additional trial from one of the flies (n=6).

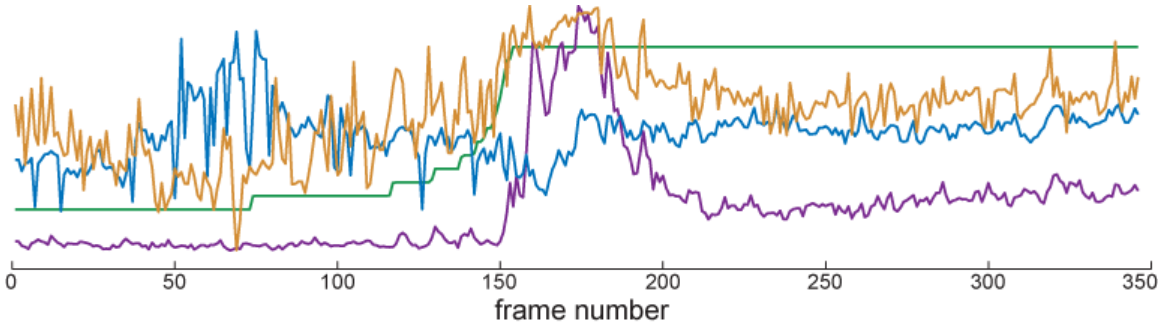

Figure IV-9: Phase-locked haltere stroke position is correlated with wingbeat amplitude during visually elicited saccades. For the single trial shown here, the orange trace shows the time course of the haltere stroke position, the purple indicates L WBA, the blue denotes R WBA, and the green is the stimulus size. The scale of the ordinate axis is arbitrary, but the two WBA signals are scaled together. The average wingbeat frequency during this trial was 244 Hz, with one video frame captured per wingstroke.

Next, I used cross-correlational analysis to determine the relative timing of changes in haltere stroke amplitude and wingbeat amplitude. I temporally shifted the haltere stroke angle and wingbeat amplitude signals and calculated the cross-covariance between the two at each shifted position. These data show that the right haltere stroke amplitude is most strongly correlated with the left wingbeat amplitude, and hardly coupled with the right wingbeat amplitude (Figure IV-10). However, the highest correlation was observed at a temporal delay near 0 ms, indicating that modulations in both signals occurred simultaneously. Another possible way to ascertain whether the haltere and wing strokes are altered together or whether haltere modulation causes wing modulation is the correlation at different frequencies. If the two systems are affected together by descending input, the coupling should be constant across frequency bands. On the other hand, if they are indirectly linked, as through a feedback network, one might expect to find stronger correlation at low frequencies than at high frequencies. I compared the correlation coefficients calculated from the same data after filtering with one of several bandpass, high-order, elliptic filters and found that most of the

observed coupling occurs between 2 and 5 Hz (Figure IV-11), suggesting but not conclusively demonstrating that the haltere and wing may be linked through feedback rather being simultaneously modulated by descending commands. This low-frequency coupling was slightly reduced during non-saccadic as opposed to saccadic flight sequences, further implying differences in the underlying control mechanisms.

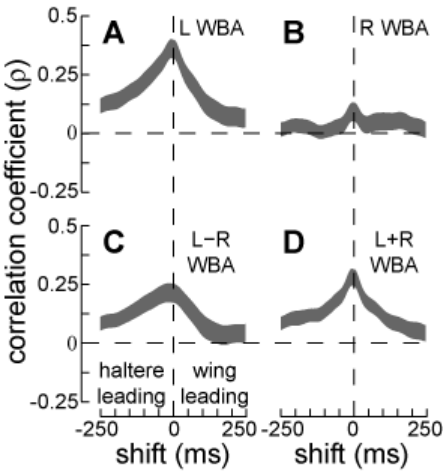

Figure IV-10: Haltere stroke position is maximally correlated with left wingbeat amplitude (L WBA). For each trial, the phase-locked haltere position was temporally shifted relative to the signal and the cross-covariance calculated. The envelopes here show the mean±s.e.m. at each shift position across all digitized trials for the haltere stroke position *versus* **(A)** L WBA, **(B)** R WBA, **(C)** L−R WBA, and **(D)** L+R WBA. Negative shift values indicate that changes in haltere stroke position occurred before changes in wingbeat amplitude. N=10 flies, n=50 trials.

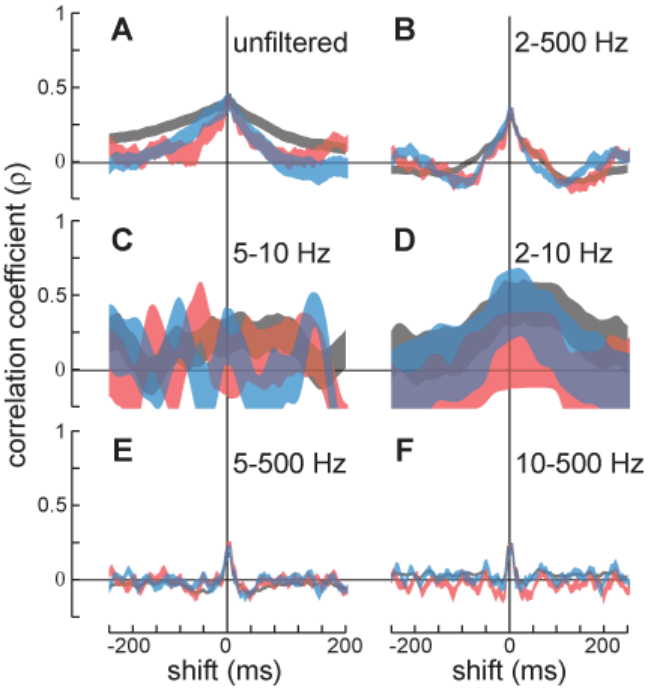

Figure IV-11: Correlation between right haltere and left wingstroke phase is highest at low frequencies. **(A-F)** Cross-covariance analysis as in Figure IV-10 was performed after bandpass-filtering with a high-order, elliptic filter for the given frequency range. Black: all data (same as Figure IV-10A; N=10 flies, n=50 trials); blue: data during visually elicited saccades only (N=5, n=14); red: data from initial non-saccadic flight during trials in which at least the first 67 frames did not contain a saccade (N=7, n=16).

V. Saccade Termination

Once a saccade has been triggered by visual or other input, multiple hypotheses could explain the observed time course of the behavior. Possibly the simplest is that the saccade completes a stereotyped time course, with neural or kinematic noise leading to a distribution of saccade dynamics. However, if the saccadelike turns performed by rigidly tethered flies are underlain by the same neural processes, this hypothesis cannot be fully true, as saccades in rigidly tethered flies have a much longer duration than in free flight (500 ms instead of 50) and such flies never produce countertorque. This leads to a second hypothesis, which is that sensory feedback, presumably from modalities not engaged on a rigid tether, gives rise to the differences between saccades in free and tethered flight, and therefore has a role in terminating the saccade motor program. It is likely, of course, that the behavior contains both feed-forward and feedback components, because otherwise a saccade by a rigidly tethered fly might never terminate. The visual system has great importance to flies (for a small cross-section of the literature, see Reichardt, 1969; Collett and Land, 1975; Götz, 1975; Reichardt and Poggio, 1976; Heisenberg and Wolf, 1984; Borst and Egelhaaf, 1989; Wolf and Heisenberg, 1990; Tammero and Dickinson, 2002a; Egelhaaf et al., 2002; Higgins, 2004; Frye and Dickinson, 2004b), so it is reasonable to test its role during saccades. The gyroscopic halteres are another likely candidate to provide feedback during saccades because of their very fast responses (Fayyazuddin and Dickinson, 1996; Sherman and Dickinson, 2003).

Therefore, I tried to quantify the relative contributions of feedback from the visual system, the halteres, and elements of feed-forward control to the time course of saccades.

Chapter Contents

Experimental Manipulations

Artificial visual feedback

In experiments designed to alter the visual feedback received during a saccade, each trial consisted of a spontaneous saccade made by the fly on the magnetic tether, at least 1 s after the previous trial. The arena displayed a pattern of vertical stripes with a fundamental spatial frequency of 22.5° in the azimuthal plane, which I refer to as the “background.” This frequency was chosen from open-loop experiments to maximize the fly's syndirectional optomotor response to stripes rotated for blocks of 10 s at an angular velocity of about $64°\cdot s^{-1}$ (Figure V-1). Between blocks, the stripes were stationary for 10 s. The observed maximum

response at a spatial frequency of 22.5° (2 pixels light, 2 pixels dark) agrees with the theoretical prediction that the strongest stimulus should be one in which the stripe width is twice the interommatidial distance of 4.6° (Götz, 1964; Egelhaaf et al., 1989). This has previously been demonstrated to be so, notably on a similar LED display by Sherman and Dickinson (2003).

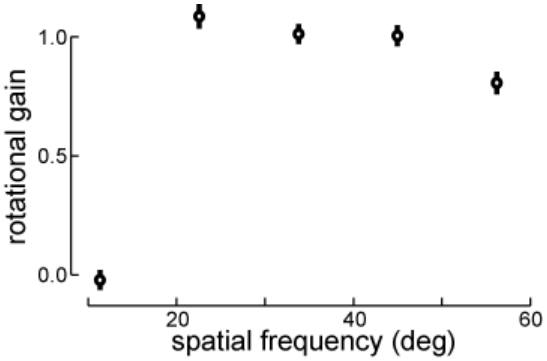

Figure V-1: Rotational optomotor response as a function of pattern spatial frequency. Frequencies tested corresponded to individual stripe widths ranging from 1 to 5 pixels in the magnetic tether arena. The calculated gain equaled the average angular velocity of the fly divided by the angular velocity of the pattern during each 10-s trial. Values are shown as mean±s.e.m. N=4 flies, n=[123, 123, 123, 125, 130] trials.

On top of these background stripes, the arena displayed a solid, dark, "foreground" stripe with a width of 45°, which could be moved independently of the background. When the fly initiated a saccade, either the foreground, background, both, or neither were rotated by 40° in 80 ms, corresponding roughly to a typical saccade in this preparation (Figure III-9). The trial type was again chosen randomly *ad hoc*, with the constraint that two consecutive trials be of different types. While the fly was not performing a saccade, the foreground stripe slowly rotated around the arena with an angular velocity that varied as the sine of its position relative to the fly's heading. This was intended to simulate the way a real object in the environment would move during the fly's forward flight, with the simplifications that the size of the object never varied and the background was stationary, but its addition did not seem to affect the flies' behavior in this paradigm.

Saccade detection in real time

For these experiments, the refresh rate of the pattern on the visual arena was increased to 220 Hz and the frame rate of the camera used to monitor behavior was raised to an average of 560 Hz. The maximum total delay was about 10 ms, therefore, between a fly's behavior and the ability of the real-time software to modify the visual stimulus in response to the fly. This corresponds to roughly two wingstrokes, or about 10–20% of the duration of a saccade in free flight. The fly-tracking software was responsible for triggering a trial when the fly spontaneously initiated a saccadic maneuver. This determination was made in real time by extracting the fly's instantaneous angular velocity between pairs of images collected at an average rate of 566 Hz (1.75 ms·frame^{-1}) and calculating the average angular velocity between each unique pair of three consecutive camera frames (e.g., the average of the instantaneous velocity between frames 1 and 2, 2 and 3, and 1 and 3, using each frame's timestamp). This estimated velocity was compared to a threshold set at 650°·s^{-1}, and a trial began when this threshold was exceeded. This procedure resulted in many “false positive” trials, when the real-time software detected a saccadic event but a *post hoc* analysis did not indicate the presence of a saccade, and fewer “false negative” trials, where a saccade revealed by *post hoc* analysis did not meet the real-time criterion. The errors between the *post hoc* determination of saccade

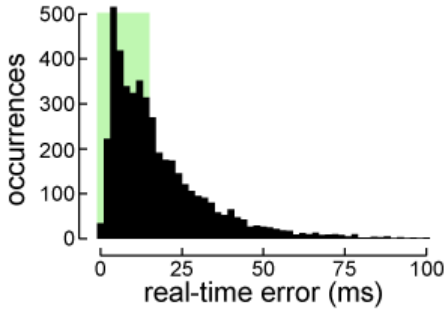

Figure V-2: Latency between real-time and *post hoc* saccade detection times. Only saccades which were detected by the real-time software between 0 and 15 ms after their true initiation time, as calculated *post hoc,* were analyzed (green box).

initiation time and the real-time trigger are shown in Figure V-2. I only analyzed trials during which both criteria were met, so that the fly both performed a saccade and triggered the real-time feedback. Additionally, only trials in which the real-time threshold was reached less than 15 ms after the *post hoc* saccade initiation time were included.

Sensory Feedback

Visual feedback

In an arena displaying a pattern of thin, vertical stripes (background) overlain by a thick, foreground stripe, either the foreground, background, both, or neither could be rapidly displaced once the fly initiated a saccade. I quantified the effects of such altered visual feedback on saccade amplitude, duration, and peak velocity (Figure V-3). The distributions of these metrics during these experiments were generally neither normal nor log-normal (Shapiro-Wilk test, $W<0.05$), so I used nonparametric statistics to test whether the median values were different (Kruskal-Wallis nonparametric one-way ANOVA with Bonferroni correction for multiple comparisons). None of these rotations of the visual environment during saccades had significant effects on saccade amplitude, duration, or peak velocity ($p>0.05$).

To test whether this effect was dependent on the exact parameters of the visual feedback used, I analyzed saccades from flies in an environment alternating between a static pattern and total darkness (see Figure II-7). The ANOVA analysis of amplitude, duration, and peak velocity suggested significant

differences between saccades in the dark and saccades in the light (Figure V-4), but these statistics depend strongly on the number of degrees of freedom (data samples). Since many more saccades were included in this calculation compared to the others presented here (i.e., this distribution was oversampled), the judgment of what *p*-value constitutes a significant difference must be more strict. Therefore, I suggest that the observed differences in saccade amplitude and peak velocity between the darkness and lit conditions are not significant, although the changes in saccade duration may be. Flies with clipped wings do not show any statistical differences between saccades in the

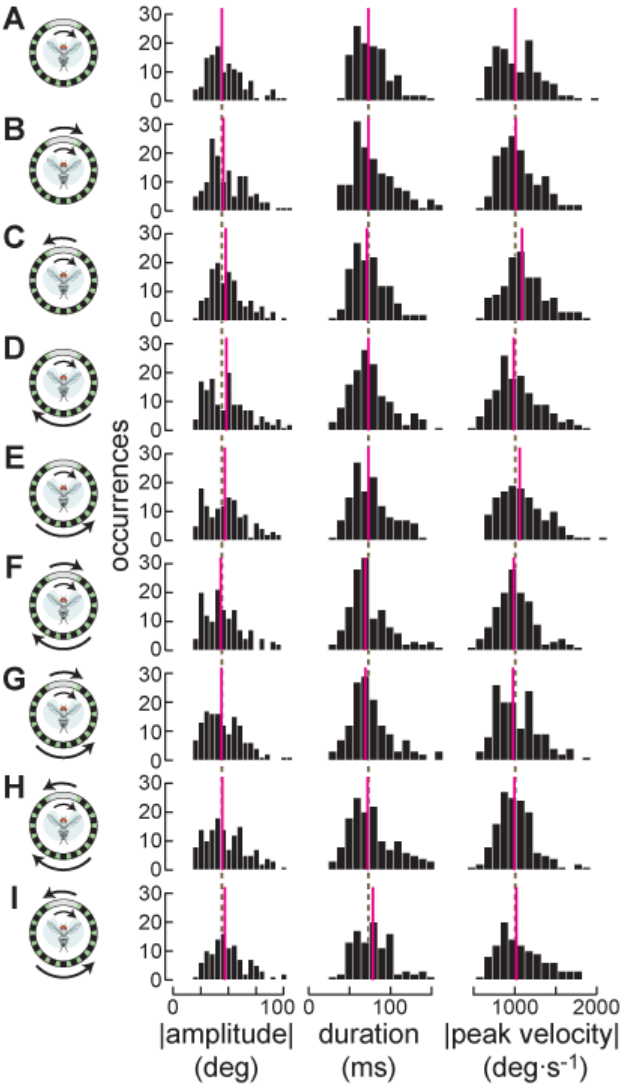

Figure V-3: Artificial visual feedback does not alter saccade dynamics. Flies were presented with a visual arena displaying 12° vertical stripes (background, or BG) behind a prominent, black, 45° vertical stripe (foreground, or FG; displayed here in light gray for clarity). During a spontaneous saccade, either the foreground, background, both, or neither was rotated by 40° in 80 ms. **(A)** No rotation (control; n=134 saccades). **(B)** Foreground rotated in the same direction as the saccade (n=151). **(C)** FG rotated against fly's turn (n=148). **(D)** Background rotated with (n=163). **(E)** BG against (n=142). **(F)** FG with/BG with (n=134). **(G)** FG with/BG against (n=141). **(H)** FG against/BG with (n=142). **(I)** FG against/BG against (n=107). None of the median values (pink bars) differed significantly from the control (Kruskal-Wallis nonparametric one-way ANOVA with Bonferroi correction for multiple comparisons; $p>0.05$). N=14 flies.

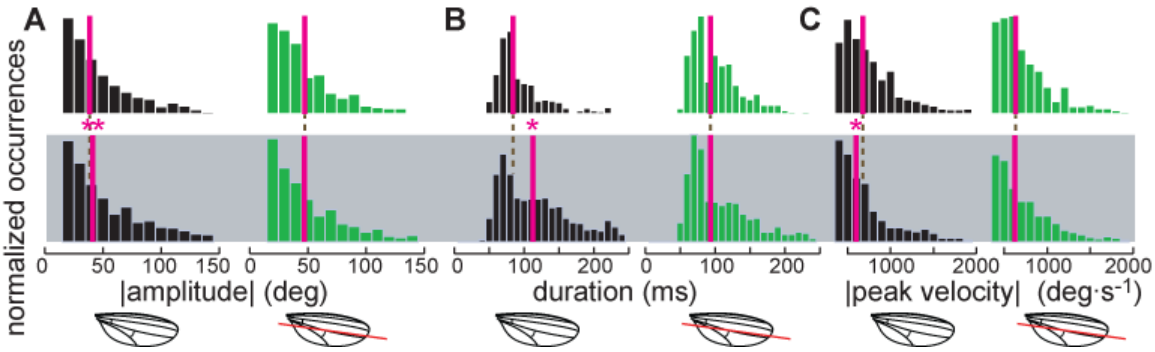

Figure V-4: Total darkness has a minimal effect on saccade dynamics (**(A)** absolute amplitude, **(B)** duration, **(C)** peak angular velocity). Top row: lit arena; bottom row: darkened arena (as in Figure II-7). N=7 intact flies (n=726 light saccades, n=629 dark); N=3 clipped flies (n=308 light, n=586 dark). Statistics as in Figure V-3 (*: $p<0.001$; **: $p<0.02$).

light and saccades in the dark, even by the less stringent criterion. Together, these results imply that the time course of saccadic turns is only minimally dependent on visual feedback.

Haltere-mediated feedback

Next, I modified the feedback received by the fly from its halteres, to determine whether they might play a role in terminating saccades. Adding mass to the endknobs of both halteres, effectively increasing the gain of the Coriolis force sensors, significantly decreased saccade amplitude and peak velocity ($p<0.001$), while tending to decrease saccade duration (Figure V-5). Ablating the left haltere, reducing the total available haltere-mediated feedback, strongly increased saccade amplitude, duration, and peak velocity ($p<0.001$). This effect was laterally symmetric, even though only one haltere had been ablated ($p>0.05$; Figure V-6), suggesting that the integration of haltere-mediated rotational feedback may be done centrally, rather than by simple, ipsilateral projections of the haltere afferent neurons. While such ipsilateral projections are present, there are ample central projections to make this interpretation plausible (Chan and

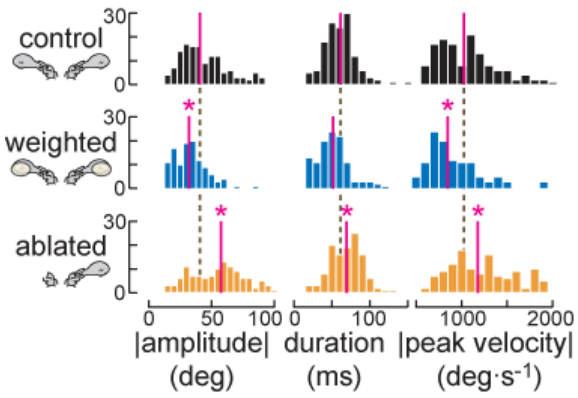

Figure V-5: Increasing or decreasing haltere-mediated feedback modifies saccade dynamics. Top to bottom: control (same data as top row of Figure V-3; N=14 flies, n=134 saccades), halteres weighted with glue droplets (N=6, n=113), left haltere ablated (N=5, n=121). Statistical analysis as in Figure V-3 (*: $p<0.001$).

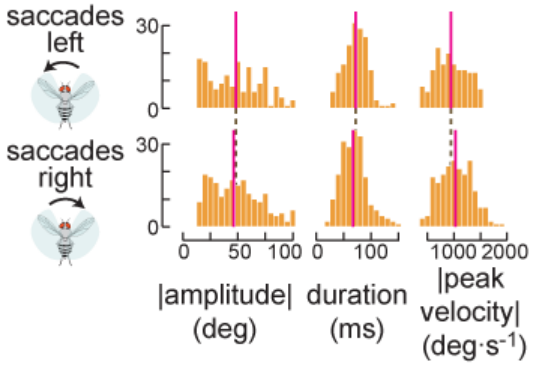

Figure V-6: The dynamics of saccades to the left and to the right are no different in flies with one haltere ablated (the left haltere). Statistics as in Figure V-3 ($p>0.05$). N=5 flies; n=166 saccades left, n=201 right.

Dickinson, 1996). I also tested crossmodal interactions, in case manipulations of the halteres unmasked some visually mediated effect. Rotating the foreground and background together, with or against the direction of a saccade, did not have any significant effects on saccade amplitude, duration, or peak velocity ($p>0.05$; Figure V-7). These results indicate that feedback from the halteres plays a major role in determining saccade dynamics.

In certain conditions, manipulations to the halteres can cause them to lose their phase alignment with the wings (von Buddenbrock, 1919; Sellke, 1936; as quoted and expanded by Pringle, 1948). Because the halteres provide stroke-by-stroke sensory feedback even in the absence of body rotation (Heide, 1983; Fayyazuddin and Dickinson, 1999), experiments that led to them being out of phase with the wings could give rise to difficulties interpreting my results. Therefore, I examined sequences of high-speed video (6000 frames·s^{-1}) from

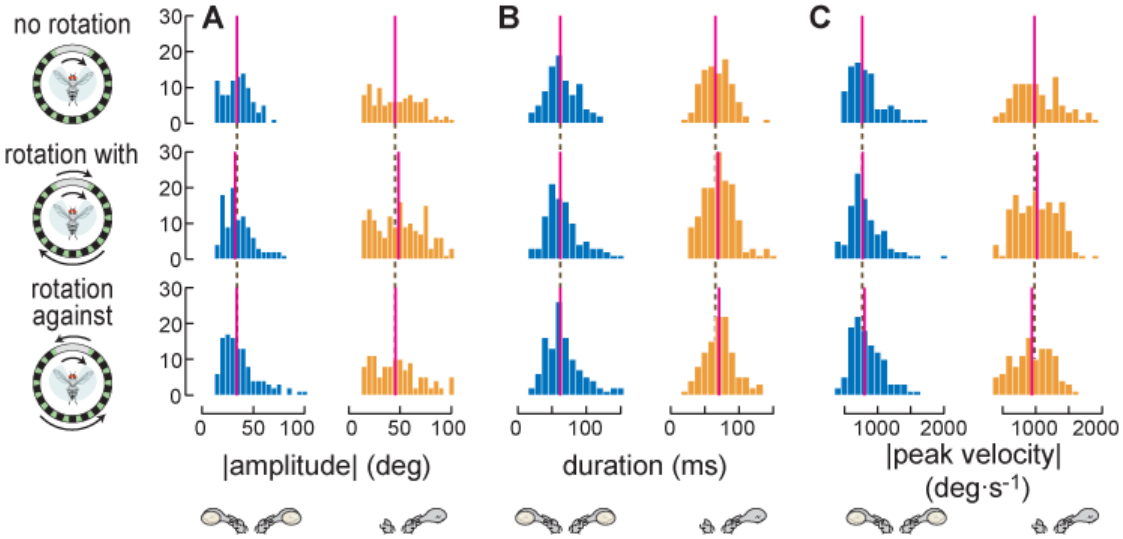

Figure V-7: The effects of visual feedback on saccade dynamics (**(A)** saccade absolute amplitude; **(B)** duration; **(C)** peak absolute velocity) do not exhibit additional crossmodal interactions in flies with haltere manipulations. N=6 flies with halteres weighted (blue histograms); N=5 flies with left haltere ablated (orange histograms). Top: no visual rotation (same data as Figure V-5), n=113 weighted saccades, n=121 ablated saccades. Middle: Foreground stripe and background pattern rotated together in the same direction as the saccade, n=130 weighted, n=187 ablated. Bottom: visual field rotated against saccade, n=137 weighted, n=121 ablated. Statistical analysis as in Figure V-3 (p>0.05).

flies with their halteres weighted (Movie V-1) or with one haltere ablated (Movie V-2). These flies exhibited no gross phase changes between wing and haltere strokes.

Clipped wings and feed-forward control

When I modified the aerodynamic surface of one of a fly's wings, saccade dynamics were altered (Figure V-8). Flies with the distal third of their left wing removed displayed smaller saccade amplitudes and peak velocities, but longer saccade durations (p<0.001). On the other hand, flies in which the posterior half of the right wing had been clipped showed decreased amplitude (p<0.001), peak velocity, and duration (p<0.02) of saccades. This was also independent of artificial visual feedback (Figure V-9; see also Figure V-4). Flies manipulated in these ways had changed their wingstroke kinematics in order to maintain a stable

heading in the face of an asymmetrical stroke-averaged moment about the yaw axis (see above), but showed no statistical differences between the amplitude, duration, or peak velocity of saccades in either direction (Figure V-10).

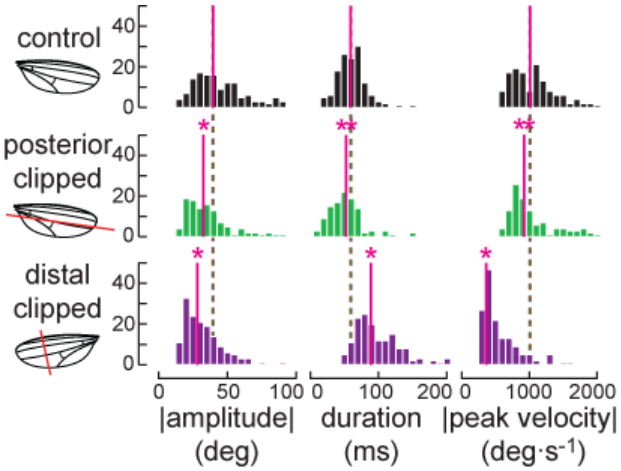

Figure V-8: Saccades are affected by changes in wing aerodynamics. Top row: control (same data as top row of Figure V-3; N=14 flies, n=134 saccades). Middle row: the posterior half of the right wing was removed (N=5, n=110). Bottom row: the distal third of the left wing was clipped (N=5, n=1292 for statistical purposes, with 150 saccades randomly selected for plotting). Statistical analysis as in Figure V-3 (*: $p<0.001$; **: $p<0.02$).

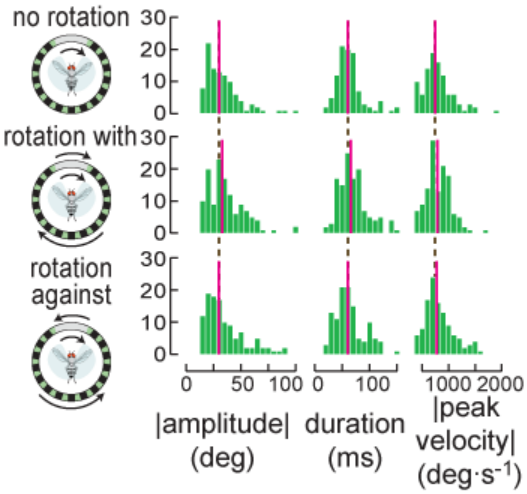

Figure V-9: Saccade dynamics are independent of visual feedback in flies with the posterior half of a wing removed. Top row: no artificial visual feedback (same data as Figure V-8; n=110 saccades). Middle: Foreground and background rotated with fly's turn (n=131). Bottom: Visual stimuli rotated against saccade (n=110). Statistics as in Figure V-3 ($p>0.05$). N=5 flies.

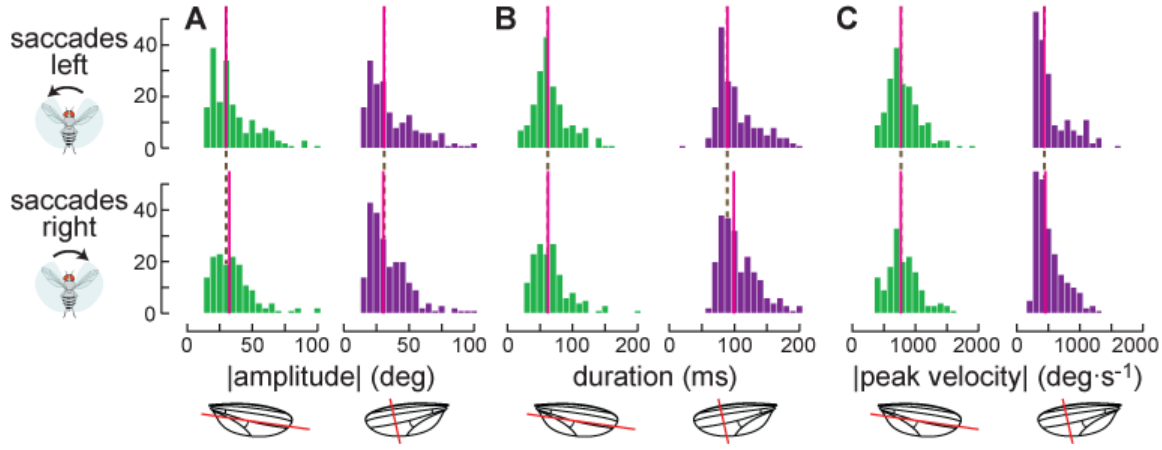

Figure V-10: Asymmetrical modification of wing surfaces does not alter saccade dynamics in one direction relative to the other (**(A)** amplitude, **(B)** duration, **(C)** peak velocity). Green histograms: posterior half of right wing removed (N=5 flies, n=184 saccades right, n=155 saccades left); purple histograms: distal third of left wing clipped (N=5, n=1128 left, n=1401 right, with 400 total saccades randomly selected for plotting here). Statistical analysis as in Figure V-3 ($p>0.05$).

VI. Discussion

I have developed a new tethered preparation of the fruit fly, in which a fly is held in place by a magnetic field but is free to rotate about one axis. Such "magnetically tethered" flies actively maintain a stable heading but also perform body saccades – rapid, stereotyped turns. Saccades can be educed by expanding visual stimuli, but visual feedback has very little influence on their time course, once initiated. Haltere-mediated feedback, on the other hand, has a strong effect on saccade dynamics, although a feed-forward component of the motor program exists, as well. My results also suggest an active role for the halteres in saccade initiation, as manipulations of the halteres affect the time course of saccades in rigidly tethered flies.

Chapter Contents

Saccades by Tethered Flies

From their first identification in rigidly tethered flies, the behaviors called "torque spikes" (Heisenberg and Wolf, 1979) or "hitches" in wingbeat amplitude (Götz et al., 1979) were tentatively equated with free flight saccades (after Land, 1973; Land and Collett, 1974; Collett and Land, 1975). However, since the duration of these tethered-flight behaviors is much longer than that of a free flight

saccade (500 ms as opposed to 50 ms; Bülthoff et al., 1980; Heisenberg and Wolf, 1984; Fry et al., 2003), and intersaccade flight trajectories are not always straight in *Drosophila* (Tammero and Dickinson, 2002a; Frye et al., 2003; also analyzed in *Calliphora* by van Hateren and Schilstra, 1999, and in *Lucilia* by Bödekker et al., 2003), it remained possible that torque spikes in rigidly tethered flies represented a behavioral pattern other than saccades. Mayer and co-workers demonstrated saccadelike behaviors in loosely tethered flies, but failed to evoke them reliably and were therefore unable to make a strong correlation with the torque spikes observed in rigidly tethered flies (Mayer et al., 1988). Tammero and Dickinson suggested that visual expansion was a cue triggering saccades as a collision-avoidance response in unrestrained flies (Tammero and Dickinson, 2002a) and found that rigidly tethered flies responded to expanding stimuli by turning away (Tammero and Dickinson, 2002b; Tammero et al., 2004) but did not claim that these reactions shared a neurobiological basis with saccades due to the difficulty in separating saccades from more gradual turns. In addition, flies in free flight must generate torque to begin a saccade and countertorque to stop turning (Fry et al., 2003), but rigidly tethered flies never do so (Heisenberg and Wolf, 1979) and loosely tethered flies were not thought to (Mayer et al., 1988).

I have bridged the gap between free and rigidly tethered flight using the magnetic tether arena, showing that magnetically tethered flies spontaneously perform saccades and that these behaviors can also be evoked by expanding visual stimuli, as they are in free flight. The duration of saccades on the magnetic

tether averages 75 ms, much more similar to free flight than to rigidly tethered flight. These saccades were slightly larger than the typical loosely tethered saccade reported by Mayer and colleagues (1988), but this could be because their actively spooled string may have introduced added frictional damping to the turns. In addition, their flies were tethered horizontally rather than at a 45° angle, and a stereotyped, three-dimensional motor pattern constrained to act about only one axis would yield different results depending on the precise axis chosen. Finally, magnetically tethered flies produce both torque and countertorque during saccades (Figure II-5), implying that the observed lack of countertorque in the rigidly tethered behaviors is due to the deprivation of haltere-mediated sensory feedback rather than to an alternate motor program. However, the estimated peak torque produced by magnetically tethered flies is only about one-eighth of that produced during a free-flight or rigidly tethered saccade (Fry et al., 2003; Heisenberg and Wolf, 1979). There are several possible explanations for this.

First, the model used to compute the torque from the body dynamics during a saccade depends on estimates of the fly's moment of inertia (I) and coefficient of friction (C) (see Equation II-2) − or more precisely, their ratio I/C, the system's time constant (τ), which could be inaccurate. However, given the observed time course of rotation, τ would have to be <0.03 s in order to reproduce the peak torque seen in free flight, and this would also predict very little countertorque at the end of a saccade. Fry and colleagues estimated $0.5<\tau<1$ s based on geometrical and kinematic analyses (Fry et al., 2003). This was thought to be an underestimate, and is unlikely to be wrong by more than an

order of magnitude. On the magnetic tether, I directly measured $\tau \approx 0.4$ s with the wings folded and $\tau \approx 0.2$ s with the wings raised, including the effects of tethering (Figure II-4). Therefore, it is unlikely that the calculated discrepancies are due an inaccurate value of the time constant.

A more probable explanation is that although the magnetic tether affords free rotation about the functional yaw axis, the halteres are only minimally sensitive to yaw rotations (Sherman and Dickinson, 2003). Therefore, the haltere-mediated feedback received by flies during magnetically tethered saccades is only partially naturalistic, which could explain some differences from the torque produced in free flight. In fact, during free flight, small pitch deflections occur within every wingstroke, as the upstroke and downstroke produce moments of pitch that generally cancel over the duration of the stroke (Fry et al., 2005). Since the halteres are most sensitive to pitch (Sherman and Dickinson, 2003), it is conceivable that the damping of this rocking motion by the magnetic field is responsible for some of the behavioral differences between free flight and magnetically tethered flight. Saccades in free flight also occur as banked turns, commonly including rotations about the yaw, pitch, and roll axes (Schilstra and van Hateren, 1999; Fry et al., 2003). In addition to excluding haltere-mediated feedback about the other axes, the kinematic effects of restricting motion to a single plane will depend on the angle of that plane relative to the body, and altering the time course of rotation necessarily affects the torque calculated by the

dynamic model. Supporting this interpretation, my data indicate an average saccade amplitude of only 35°, compared to the 90° seen during free flight (Tammero and Dickinson, 2002a; Fry et al., 2003).

Furthermore, high-speed video sequences of magnetically tethered flies performing saccades (Movie VI-1) show that the wings touch at the peak of the upstroke, a kinematic type known as the “clap-and-fling” stroke (Weis-Fogh, 1973; Götz, 1987). Among other differences from rigidly tethered flight, flies in free flight do not generally make clap-and-fling strokes (Ennos, 1989; Fry et al., 2005), which generate increased downward pitch (Fry et al., 2005; Lehmann et al., 2005) and probably interfere with the production of yaw torque (Lehmann and Dickinson, 2001). Presumably, the reason that flies demonstrate clap-and-fling strokes instead of normal wingstrokes is due to a lack of sensory feedback, from modalities disengaged or only partially engaged in flies which are rigidly or magnetically tethered. Because of these kinematic differences, an exact match to the free flight torque profile would be extremely improbable in tethered flies. On balance, therefore the preponderance of the evidence suggests that the behaviors observed on the magnetic tether, and on the rigid tether in response to similar visual stimuli, do in fact share a neurobiological basis with saccades in free flight.

Insights for Visually Guided Flight

Vision is implicated in both guidance and the stability of flight in flies (Egelhaaf et al., 1988; 2003; Egelhaaf and Kern, 2002; Sherman and Dickinson,

2003; also Figure II-7), and there is a large amount of indirect evidence for the existence of a neural implementation of the Hassenstein-Reichardt (delay-and-correlate; after Hassenstein and Reichardt, 1956) elementary motion detector (EMD) in the fly visual system. Some neurons in the lobula plate respond to pure motion stimuli (Egelhaaf et al., 1989; Borst and Egelhaaf, 1989), including specific patterns of visual motion that would appear on the retina of flying insects (Krapp and Hengstenberg, 1996; Franz and Krapp, 2000). Many details of the physiological responses of these neurons (Harris et al., 2000; Haag and Borst, 2004) and fly behavior (Borst, 1990; Schilstra and van Hateren, 1999) have been described in terms of the output of an array of EMDs. However, the firing rate of one notable motion-sensitive neuron in the locust, the descending contralateral motion detector (DCMD), has been well characterized in terms of an angular threshold model (Hatsopoulos et al., 1995; Gabbiani et al., 1999; 2001; 2002), difficult to reconcile with simple motion-sensitive responses. Neurons of both types have been described in pigeons (Sun and Frost, 1998) and moths (Wicklein and Strausfeld, 2000) and might reasonably be considered in flies, in spite of the theoretical appeal and prominence of EMD-based models for fly vision.

There are already some indications that the fly visual system might have alternate processing pathways for large-field (background) and small-object (foreground) motion (Virsik and Reichardt, 1974; 1976; Reichardt and Poggio, 1979; Egelhaaf, 1985; 1987; 1990). In particular, Reichardt and others have suggested that the neural circuitry specialized for discrimination of small-field objects does so by separating fast, relative motion from slow, coherent motion

(Reichardt et al., 1989). I tested both foreground and background rotation as possible components of visual feedback mediating saccade termination in magnetically tethered flies, but none of the combinations of this motion affected saccade dynamics. However, the probability of a statistical difference from the control condition was relatively high for the trials in which the foreground stripe was rotated against the direction of the turn (i.e., low values of p=0.15 for saccade duration, p=0.07 for peak velocity). This suggests the possibility of differential effects for foreground and background motion in the saccadic control system. It may be that the position of the stripe with respect to the fly's heading is important in this effect, but I had insufficient data to test for this possibility. Small, expanding objects can elicit landing responses (Borst and Bahde, 1986; 1988) in tethered flies, but Tammero and Dickinson demonstrated that the landing response is controlled separately from saccade initiation (Tammero and Dickinson, 2002b). They also showed that saccades can be initiated by large-field expansion in free flight (Tammero and Dickinson, 2002a), but found turning responses to expanding objects in rigidly tethered flies. My results indicate that expanding objects can reliably evoke saccades, but the effects of stimulating rigidly tethered flies with large-field motion were more equivocal (Figure IV-3).

In Chapter III, I used the time course of saccade initiation to fit the model developed by Gabbiani and colleagues for critical-angle detection based on the output of the locust DCMD neuron (Gabbiani et al., 1999). As the locust exhibits a diving behavior that is correlated with the activity of this neuron (Santer et al., 2005), it is reasonable to examine the saccadic escape response as a proxy for

neural activity in a homologous collision-avoidance circuit in the fruit fly, and this model fit my experimental data very well (Figure III-7). Although it is not clear how a network of neurons might do so (though see Gabbiani et al., 2002), if the critical-angle calculation were made by the clever combination of EMD output, what predictions would follow for the neural and behavioral responses? The Hassenstein-Reichardt theory predicts that concentrically striped stimuli, containing more “motion energy” for a given perimeter, should more strongly activate EMDs and, presumably, descending neurons. Gabbiani and co-workers (2001) observed that such stimuli led to an earlier peak response time in DCMD, although this effect was not statistically significant. Within the margin of error, my data also exhibit this trend (Figure III-7, green circle). Additionally, while the predicted response of a global motion detector to expansion along only one visual axis would be reduced relative to a two-dimensional stimulus, presumably in proportion to the reduction in motion energy, the response of an angular threshold circuit would depend on the manner of the system's construction, and could be reduced or unaffected. Fruit flies show a much later peak in saccade initiation probability when presented with such one-dimensional expansion stimuli (Figure III-7, orange circles), consistent with either model but indicating that an angular size calculation, if present, is not made along only one axis. Corroborating this, Tammero and Dickinson found saccade responses to full-field visual expansion in freely flying *Drosophila* (Tammero and Dickinson, 2002a). Guest and Gray found, however, that DCMD exhibits strongly sublinear summation when multiple, looming objects are presented (Guest and Gray, 2006), suggesting that some

EMD-related effects may be biophysically filtered during pre-DCMD neural processing. Another effect that Tammero and Dickinson suggested was an ambiguity about whether flies avoid expansion or fixate contraction (Tammero et al., 2004). I found that flies did sometimes decrease their saccade probability in response to contraction of a visual object, suggesting that both types of responses may exist. During artificial perturbations such as might occur in free flight, e.g., sideslip due to wind, expansion and contraction co-occur at opposite poles of the visual field, and therefore both responses act in concert, but in experimental conditions additional details differentiating the two may be investigated.

In any case, although my data show that visual feedback is important in stabilizing straight flight, they demonstrate only a minor effects of vision in the control of saccades, once initiated. Because of the strong visual response to rotational motion (Götz, 1964; Buchner, 1976; Blondeau and Heisenberg, 1982; Sherman and Dickinson, 2003; see also Figure IV-8; Figure V-1), one hypothesis might be that this response is inhibited by corollary discharge during saccades. To test this, I analyzed the flight behavior during the “false positive” trials, in which the visual feedback sequence was initiated but no saccade was indicated by a *post hoc* analysis. In these trials, flies reacted to a full-field visual rotation with an average syndirectional turn of 2-3°, similar to the statistically insignificant changes in saccade amplitude seen in response to the same stimuli during saccades. This suggests that the duration of visual feedback during a saccade is too brief to elicit a substantial turning response. Heisenberg and Wolf obtained contradictory

results, in which they reported a response to saccade-triggered artificial visual feedback (Heisenberg and Wolf, 1979; 1984). Aside from statistical issues because this finding was based on a very few trials ($n<10$), this may be due to the fact that those authors presented flies with longer and slower rotations of 30° in 200 ms ($150°\cdot s^{-1}$), while in my experiments involved visual rotation amounting to 40° in 80 ms ($500°\cdot s^{-1}$). Furthermore, it has been shown that visual feedback information is partially deprecated in favor of haltere-mediated rotational feedback, if present (Sherman and Dickinson, 2004), as is the case on the magnetic tether.

The Halteres during Saccades

The precise role of the halteres during both the initiation and ongoing control of saccades remain uncertain. Although there are many possible mechanisms through which the halteres might be involved in saccade generation, two distinct hypotheses have been advanced that are difficult to discriminate experimentally, which I will refer to as the “efferent inhibition” and “efferent activation” models. The first hypothesis is that the predicted haltere input is nullified through an efference copy (efferent inhibition) mechanism whereby the haltere steering muscles are used to counteract the reafferent signals generated during a turn. This is distinguished from a closely related, corollary discharge mechanism, in which the haltere afferent neurons or their downstream targets would be inhibited. A corollary discharge could occur, but electrophysiological recordings from haltere afferents, muscles, and wing muscles and motor neurons

have not found evidence of this during saccades (Lehmann and Götz, 1996; Lehmann and Dickinson, 1997; Fayyazuddin and Dickinson, 1996; 1999; Chan et al., 1998; Balint and Dickinson, 2001; 2004). The second scenario also involves descending motor commands to the haltere steering muscles, which in this case are used to deflect the haltere from its stroke plane, mimicking the effects of an angular rotation of the body (proposed by Chan et al., 1998). The afferent, mechanosensory pathway which normally acts to sense and counter imposed rotations (Pringle, 1948; Nalbach and Hengstenberg, 1994; Fayyazuddin and Dickinson, 1999; Dickinson, 1999; Sherman and Dickinson, 2003) is thus activated by efferent input (the “efferent activation” hypothesis). One advantage of this scheme is that afferent signals from the halteres are phase-locked to the wingstrokes by default (Fayyazuddin and Dickinson, 1999), whereas descending commands may not be, and the effects of commands to the wing steering muscles depend strongly on their precise timing in the wingstroke phase (Lehmann and Götz, 1996; Tu and Dickinson, 1996; Balint and Dickinson, 2001; 2004). It is known that muscles in the neck are electrically coupled to haltere afferent neurons (Sandeman, 1980; Sandeman and Markl, 1980; Strausfeld and Seyan, 1985), as the wing steering muscles are (Chan and Dickinson, 1996), and head rotation in rigidly tethered *Calliphora* (Nalbach and Hengstenberg, 1994) and *Drosophila* (Reiser, 2006) is coordinated with turning responses. Parsimoniously, this suggests that muscles in both the neck and the wings may be driven by the halteres, rather than all three systems being controlled by descending neurons.

However, to date, it is still unknown whether motion of the halteres is actively modulated in any way during flight, as both of these models would require. As evolutionarily modified hindwings, the halteres are equipped with steering muscles which are serially homologous to the steering muscles of the (fore)wings (Bonhag, 1949). Contraction of the haltere steering muscles would presumably be responsible for any active modulation of their strokes. In the blowfly *Calliphora*, it has been shown that the haltere steering muscles respond to visual motion (Chan et al., 1998), but, although they are presumably similar, even the existence of these muscles in *Drosophila* has not yet been demonstrated. I have begun anatomical characterization of fruit flies genetically engineered to express muscular myosin tagged with green fluorescent protein, which will allow relatively simple visualization of the thoracic musculature, but these studies are still in progress. It is also possible that the motion of the halteres could be mechanically modified by other muscles acting on the thoracic wall; in fact, the entire downstroke of the haltere is known to be actuated by passive properties of the cuticle (Pringle, 1948; 1949). My observation that weighting the halteres alters saccade dynamics provides no direct or mechanistic evidence, but implies an active role for the halteres in saccade initiation because no rotation or Coriolis forces were experienced by these rigidly tethered flies.

Assuming that the fly is capable of directly modulating its haltere-mediated input, one possible way to discriminate between these two suggested functions of the halteres (efferent inhibition or efferent activation) is by the relative timing of changes in kinematics between the wings and the halteres. If alterations in the

haltere strokes can be observed before changes in the wingstrokes, this could be evidence that the halteres are modulated first and then act to drive modification of wingstroke kinematics, supporting the efferent activation model. As a first step toward testing this timing hypothesis, I developed a preparation in which video images of the haltere were collected at a constant phase relationship to the wing. My preliminary results from this investigation indicate that the phase of the right haltere stroke relative to the left wingstroke is altered during turns (Chapter III). The interpretation of these data is still somewhat clouded, however, because collection of the video images was phase-locked to a point during the downstroke of the left wing. Therefore, an explanation for this observation that cannot be dismissed is that the right haltere stroke is perfectly phase-locked to the right wing but that the phase relationship of the two wings changes during active maneuvers. It is certainly clear that the right and left wingbeat kinematics differ during turns (Götz, 1968; Dickinson et al., 1993; Fry et al., 2003; Balint and Dickinson, 2004), but even the most extreme experimental manipulations left the wing upstrokes and downstrokes fully synchronized, which is to be expected because the main forces used to power the strokes are generated by a deformation of the entire thorax (Dickinson and Tu, 1997).

Additional experiments using the right wing as a video-capture trigger and utilizing images taken at different stroke phases may help to answer whether the wings and halteres are modulated together or independently. Experimentally, the range of phases at which the halteres can be observed is somewhat limited by the motion of the wings, as from the camera angle I used, the wings obscure the

haltere during (haltere) downstroke, and the body conceals the haltere from many other camera positions. Additionally, the analysis described here is only capable of extracting a phase difference between the wings and halteres, but if the haltere steering muscles truly simulate the effects of an angular rotation, they must cause a deflection of the haltere from its stroke plane as Coriolis forces would (Fraenkel and Pringle, 1938; Pringle, 1948; Nalbach, 1993). This is also challenging to visualize in practice; as the Coriolis forces are dependent on haltere velocity (see Figure I-2), they are maximal during phases when the wings almost totally conceal the halteres (Nalbach, 1993; 1994). I made some attempts to position the camera to capture changes in the haltere stroke plane, but I did not find a camera angle which revealed these. Finally, digitization of the haltere position for every wingstroke is an incredibly labor-intensive process. Computer vision has long offered hope for automation of similar tasks, but it has not yet fully delivered, especially for images with contrast levels as low as in those collected during these experiments. Increasing the light levels is possible, but even the flies from which data is presented here exhibited negative phototaxis during the periods when the strobed LEDs were active, more likely due rather to heat than the red (invisible) light. Although this should not affect wing-haltere coupling or saccades, once initiated, it was sometimes quite pronounced even during the 5 s between stimulations in early experiments, leading me to later increase the intertrial interval.

Therefore, it remains to be definitively determined whether the haltere is modulated relative to its ipsilateral wing, and if so, whether they are modulated

together or if the haltere is driving the wing. In the end, a definitive case for differentiating between the two proposed models of haltere function during saccades will likely require electrophysiological recordings from descending, command neurons and in the wing and haltere steering muscles. Unfortunately, due to simple constraints of size, neural recordings are very difficult to achieve in *Drosophila*. It is known that some of the largest changes in wing steering muscle activity during saccades occur in the first and second basalar muscles (b1 and b2; Heide and Götz, 1996). The haltere contains several mechanoreceptive fields (Chevalier, 1966; Grünert and Gnatzy, 1987), and only two of these − the df2 campaniform sensillum and the chordotonal organ − are thought to be sensitive to Coriolis forces (Pringle, 1948; Fayyazuddin and Dickinson, 1996). Afferent projections from the df2 campaniform field drive activity in the b1 muscle's motor neuron through a mixed chemical/electrical synapse (Fayyazuddin and Dickinson, 1996; Trimarchi and Murphey, 1997). The other campaniform sensilla respond to every stroke of the haltere, and therefore provide wingbeat-synchronous input that drives the wing steering muscles in the absence of body rotation (Heide, 1983). Therefore, the haltere ablation experiments I performed must be interpreted with caution. Flies with one haltere removed show an overall increase in wingbeat frequency (Dickinson, 1999; also Figure IV-5) and seem to have difficulty regulating wingstroke amplitude on the ipsilateral side. This suggests that the wing steering muscles are still entrained by haltere-synchronous input in these flies, but activation of the haltere afferent neurons is no longer phase-locked to the wingbeats. Flies with one haltere are capable of free flight, however

(Fraenkel, 1939), but flies with both halteres ablated are not, an observation attributed first to Derham (1713). Flies with bilateral haltere ablations also will not sustain flight on the magnetic tether for more than a few minutes at most, and their saccades and flight dynamics appear highly distorted. Such flies will maintain flight for several minutes in total darkness, however, comparable to intact flies (data not shown; see also Heisenberg and Wolf, 1984). It is theoretically possible to genetically ablate only the Coriolis-sensitive, df2 campaniform sensillum while leaving the rest of the haltere intact, but no genetic markers specific to this sensory field have yet been described. The mutant *shaking-B*^{2} lacks functional gap junction proteins in many parts of its body (Thomas and Wyman, 1984), including the synapses between the halteres and wing motor neurons (Trimarchi and Murphey, 1997). Magnetically tethered flies carrying this mutation performed similarly to flies with both halteres ablated. However, they did appear to perform saccades in total darkness, and although sufficient data were not gathered to enable a comparison with my other results, this strain should be included in future studies.

It now appears that a major determinant of saccade magnitude comes *via* feedback from the halteres. Adding mass to the haltere endknobs, effectively increasing the Coriolis forces sensed by the halteres, leads to smaller saccades in magnetically tethered flies. Conversely, ablation of one haltere, decrementing the total haltere-mediated feedback received by the fly, yields larger, longer saccades in a laterally symmetric fashion. This is consistent with a hypothesis that the saccade behavior is terminated by a threshold of summed rotational

information from the halteres. However, the fact that changes in the aerodynamic efficacy of the wings modify the output of the saccade motor program indicates that saccades may include an element of feed-forward control, and that sensory feedback (such as from the halteres) is insufficient to compensate for large alterations of the saccade effectors. The same experimental manipulations of the halteres that I performed on magnetically tethered flies had very different effects on rigidly tethered animals: weighting the halteres decreased saccade magnitude on the magnetic tether, but increased it on the rigid tether. As rigidly tethered flies experienced no passive stimulation of the halteres, these data suggest that an active process in the halteres is involved in saccade initiation, of unknown nature but which is enhanced by extra weight, and the saccade motor program is terminated by passive haltere sensation of rotational motion, which is also amplified by additional haltere mass. However, the increase in haltere-mediated rotational feedback must be greater than the augmentation of the initiation sequence.

In any case, these results constitute additional evidence against the existence of a blanket corollary discharge inhibition of haltere reafference during saccades, but do not preclude an efference copy mechanism in which a quantitatively matched, sign-reversed copy of the predicted input from a motor command is added to the actual afferent input during an action. If this were the case, a strengthening of the efferent signal used to initiate a saccade would make the fly turn more vigorously than normal because of larger errors between the expected and actual turning feedback. Conversely, increasing the amount of

rotation perceived by the halteres would lead to an earlier termination of the saccade motor program. A non-quantitative efference copy is equivalent to a complete inhibition of haltere function during saccades, which is not supported by my data. Thus, the efference inhibition proposal for haltere function could explain my results, but the efference activation model, in which the halteres are actively used to initiate a turn, can only do so if additional weight on the haltere endknobs would lead to a larger active deflection of the halteres. It seems more likely that the haltere steering muscles would have less effect on the haltere strokes if the halteres were more massive, but this would lead to smaller saccades in rigidly tethered flies with weighted halteres. However, additional experiments, likely involving electrophysiology, will be required to definitively determine which, if either, of these two provocative hypotheses is correct.

VII. Bibliography

Autrum, H. (1958). Electrophysiological analysis of the visual systems in insects. *Exp Cell Res Suppl* **14**, 426-439. [Medline]

Bahill, A. T., Clark, M. R. and Stark, L. (1975). The main sequence: A tool for studying eye movements. *Math Biosci* **24**, 191-204. [DOI: 10.1016/0025-5564(75)90075-9]

Balint, C. N. and Dickinson, M. H. (2001). The correlation between wing kinematics and steering muscle activity in the blowfly *Calliphora vicina*. *J Exp Biol* **204**, 4213-4226. [Journal]

Balint, C. N. and Dickinson, M. H. (2004). Neuromuscular control of aerodynamic forces and moments in the blowfly, *Calliphora vicina*. *J Exp Biol* **207**, 3813-3838. [DOI: 10.1242/jeb.01229

Bender, J. A. and Dickinson, M. H. (2006a). Visual stimulation of saccades in magnetically tethered *Drosophila*. *J Exp Biol* **209**, 3170-3182. [DOI: 10.1242/jeb.02369]

Bender, J. A. and Dickinson, M. H. (2006b). A comparison of visual and haltere-mediated feedback in the control of body saccades in *Drosophila melanogaster*. *J Exp Biol* **209**, 4597-4606. [DOI: 10.1242/jeb.02583]

Bernhard, C. G. and Ottoson, D. (1960). Comparative studies on dark adaptation in the compound eyes of nocturnal and diurnal Lepidoptera. *J Gen Physiol* **44**, 195-203. [Journal]

Blondeau, J. and Heisenberg, M. (1982). The 3-dimensional optomotor torque system of *Drosophila melanogaster* – studies on wildtype and the mutant *optomotor-blind*^{h31}. *J Comp Physiol A Sens Neural Behav Physiol* **145**, 321-329. [DOI: 10.1007/BF00619336]

Böddeker, N., Kern, R. and Egelhaaf, M. (2003). Chasing a dummy target: Smooth pursuit and velocity control in male blowflies. *Proc Royal Soc London B Biol Sci* **270**, 393-399. [DOI: 10.1098/rspb.2002.2240]

Bonhag, P. F. (1949). The thoracic mechanism of the adult horsefly (Diptera: Tabanidae). *Cornell Univ Ag Exp Station Mem* **285**, 3-39.

Borst, A. (1986). Time course of the houseflies' landing response. *Biol Cybern* **54**, 379-383. [DOI: 10.1007/BF00355543]

Borst, A. (1990). How do flies land? *BioScience* **40**, 292-299. [JSTOR]

Borst, A. and Bahde, S. (1986). What kind of movement detector is triggering the landing response of the housefly? *Biol Cybern* **55**, 59-69. [DOI: 10.1007/BF00363978]

Borst, A. and Bahde, S. (1988). Visual information-processing in the fly's landing system. *J Comp Physiol A Sens Neural Behav Physiol* **163**, 167-173. [DOI: 10.1007/BF00612426]

Borst, A. and Egelhaaf, M. (1989). Principles of visual motion detection. *Trends Neurosci* **12**, 297-306. [DOI: 10.1016/0166-2236(89)90010-6]

Buchner, E. (1976). Elementary movement detectors in an insect visual system. *Biol Cybern* **24**, 85-101. [DOI: 10.1007/BF00360648]

Bülthoff, H., Poggio, T. and Wehrhahn, C. (1980). 3-D analysis of the flight trajectories of flies (*Drosophila rnelanogaster*). *Z Naturforsch* **35c**, 811-815.

Chan, W. P. and Dickinson, M. H. (1996). Position-specific central projections of mechanosensory neurons on the haltere of the blow fly, *Calliphora vicina*. *J Comp Neurol* **369**, 405-418. [DOI: 10.1002/(SICI)1096-9861(19960603)369:3<405::AID-CNE6>3.0.CO;2-9]

Chan, W. P., Prete, F. and Dickinson, M. H. (1998). Visual input to the efferent control system of a fly's "gyroscope." *Science* **280**, 289-292. [DOI: 10.1126/science.280.5361.289]

Chevalier, R. L. (1969). The fine structure of campaniform sensilla on the halteres of *Drosophila melanogaster*. *J Morphol* **128**, 443-463. [DOI: 10.1002/jmor.1051280405]

Cole, E. S. and Palka, J. (1982). The pattern of campaniform sensilla on the wing and haltere of *Drosophila melanogaster* and several of its homeotic mutants. *J Embryol Exp Morphol* **71**, 41-61. [Medline]

Collett, T. S. and Land, M. F. (1975). Visual control of flight behavior in hoverfly, *Syritta pipiens* L. *J Comp Physiol A Sens Neural Behav Physiol* **99**, 1-66. [DOI: 10.1007/BF01464710]

David, C. T. (1978). Relationship between body angle and flight speed in free-flying *Drosophila*. *Physiol Ent* **3**, 191-195.

Derham, W. (1713). *Physico-theology: Or, a Demonstration of the Being and Attributes of God, from his Works of Creation.* London: W. Innys.

Dickinson, M. H. (1990). Comparison of encoding properties of campaniform sensilla on the fly wing. *J Exp Biol* **151**, 245-261. [Journal]

Dickinson, M. H. (1999). Haltere-mediated equilibrium reflexes of the fruit fly, *Drosophila melanogaster*. *Phil Trans Royal Soc London B Biol Sci* **354**, 903-916. [DOI: 10.1098/rstb.1999.0442]

Dickinson, M. H., Lehmann, F.-O. and Götz, K. G. (1993). The active control of wing rotation by *Drosophila*. *J Exp Biol* **182**, 173-189. [Journal]

Dickinson, M. H., Lehmann, F.-O. and Sane, S. P. (1999). Wing rotation and the aerodynamic basis of insect flight. *Science* **284**, 1954-1960. [DOI: 10.1126/science.284.5422.1954]

Dickinson, M. H. and Lighton, J. R. (1995). Muscle efficiency and elastic storage in the flight motor of *Drosophila*. *Science* **268**, 87-90. [DOI: 10.1126/science.7701346]

Dickinson, M. H. and Tu, M. S. (1997). The function of dipteran flight muscle. *Comp Biochem Physiol A Physiol* **116**, 223-238. [DOI: 10.1016/S0300-9629(96)00162-4]

Dickson, W. B., Straw, A. D., Poelma, C. and Dickinson, M. H. (2006). An integrative model of insect flight control. In *44th AIAA Aerospace Sciences Meeting and Exhibit*. Reno, NV; USA.

Egelhaaf, M. (1985). On the neuronal basis of figure-ground discrimination by relative motion in the visual system of the fly. *Biol Cybern* **52**, 123-140. [DOI: 10.1007/BF00364003]

Egelhaaf, M. (1987). Dynamic properties of two control systems underlying visually guided turning in house-flies. *J Comp Physiol A Sens Neural Behav Physiol* **161**, 777-783. [DOI: 10.1007/BF00610219]

Egelhaaf, M. (1990). Spatial interactions in the fly visual system leading to selectivity for small-field motion. *Naturwissenschaften* **77**, 182-185. [DOI: 10.1007/BF01131163]

Egelhaaf, M., Böddeker, N., Kern, R., Kretzberg, J., Lindemann, J. P. and Warzecha, A. K. (2003). Visually guided orientation in flies: Case studies in computational neuroethology. *J Comp Physiol A Neuroethol Sens Neural Behav Physiol* **189**, 401-409. [DOI: 10.1007/s00359-003-0421-3]

Egelhaaf, M., Borst, A. and Reichardt, W. (1989). The nonlinear mechanism of direction selectivity in the fly motion detection system. *Naturwissenschaften* **76**, 32-35. [DOI: 10.1007/BF00368311]

Egelhaaf, M., Hausen, K., Reichardt, W. and Wehrhahn, C. (1988). Visual course control in flies relies on neuronal computation of object and background motion. *Trends Neurosci* **11**, 351-358. [DOI: 10.1016/0166-2236(88)90057-4]

Egelhaaf, M. and Kern, R. (2002). Vision in flying insects. *Curr Opin Neurobiol* **12**, 699-706. [DOI: 10.1016/S0959-4388(02)00390-2]

Egelhaaf, M., Kern, R., Krapp, H. G., Kretzberg, J., Kurtz, R. and Warzecha, A. K. (2002). Neural encoding of behaviourally relevant visual-motion information in the fly. *Trends Neurosci* **25**, 96-102. [DOI: 10.1016/S0166-2236(02)02063-5]

Ennos, A. R. (1989). The kinematics and aerodynamics of the free flight of some Diptera. *J Exp Biol* **142**, 49-85. [Journal]

Fayyazuddin, A. and Dickinson, M. H. (1996). Haltere afferents provide direct, electrotonic input to a steering motor neuron in the blowfly, *Calliphora*. *J Neurosci* **16**, 5225-5232. [Journal]

Fayyazuddin, A. and Dickinson, M. H. (1999). Convergent mechanosensory input structures the firing phase of a steering motor neuron in the blowfly, *Calliphora*. *J Neurophysiol* **82**, 1916-1926. [Journal]

Fermi, G. and Reichardt, W. (1963). Optomotorische Reaktionen tier Fliege *Musca domestica*. *Kybernetik* **2**, 15-28. [DOI: 10.1007/BF00292106]

Fraenkel, G. (1939). The function of the halteres of flies (Diptera). *Proc Zool Soc London A Gen Exp* **109**, 69-U14.

Fraenkel, G. and Pringle, J. W. S. (1938). Halteres of flies as gyroscopic organs of equilibrium. *Nature* **141**, 919-920.

Franz, M. O. and Krapp, H. G. (2000). Wide-field, motion-sensitive neurons and matched filters for optic flow fields. *Biol Cybern* **83**, 185-197. [DOI: 10.1007/s004220000163]

French, A. S. (1980). Phototransduction in the fly compound eye exhibits temporal resonances and a pure time delay. *Nature* **283**, 200-202. [DOI: 10.1038/283200a0]

Fry, S. N., Sayaman, R. and Dickinson, M. H. (2003). The aerodynamics of free-flight maneuvers in *Drosophila*. *Science* **300**, 495-498. [DOI: 10.1126/science.1081944]

Fry, S. N., Sayaman, R. and Dickinson, M. H. (2005). The aerodynamics of hovering flight in *Drosophila*. *J Exp Biol* **208**, 2303-2318. [DOI: 10.1242/jeb.01612]

Frye, M. A. and Dickinson, M. H. (2004a). Motor output reflects the linear superposition of visual and olfactory inputs in *Drosophila*. *J Exp Biol* **207**, 123-131. [DOI: 10.1242/jeb.00725]

Frye, M. A. and Dickinson, M. H. (2004b). Closing the loop between neurobiology and flight behavior in *Drosophila*. *Curr Opin Neurobiol* **14**, 729-736. [DOI: 10.1016/j.conb.2004.10.004]

Frye, M. A., Tarsitano, M. and Dickinson, M. H. (2003). Odor localization requires visual feedback during free flight in *Drosophila melanogaster*. *J Exp Biol* **206**, 843-855. [DOI: 10.1242/jeb.00175]

Fukushima, K. and Kaneko, C. R. S. (1995). Vestibular integrators in the oculomotor system. *Neurosci Res* **22**, 249-258. [DOI: 10.1016/0168-0102(95)00904-8]

Fuortes, M. G. and Hodgkin, A. L. (1964). Changes in time scale and sensitivity in the ommatidia of *Limulus*. *J Physiol* **172**, 239-263. [PubMed]

Gabbiani, F., Krapp, H. G., Koch, C. and Laurent, G. (2002). Multiplicative computation in a visual neuron sensitive to looming. *Nature* **420**, 320-324. [DOI: 10.1038/nature01190]

Gabbiani, F., Krapp, H. G. and Laurent, G. (1999). Computation of object approach by a wide-field, motion-sensitive neuron. *J Neurosci* **19**, 1122-1141. [Journal]

Gabbiani, F., Mo, C. H. and Laurent, G. (2001). Invariance of angular threshold computation in a wide-field looming-sensitive neuron. *J Neurosci* **21**, 314-329. [Journal]

Gnatzy, W., Grünert, U. and Bender, M. (1987). Campaniform sensilla of *Calliphora vicina* (Insecta, Diptera). 1. Topography. *Zoomorphol* **106**, 312-319. [DOI: 10.1007/BF00312005]

Goodman, L. J. (1960). The landing responses of insects. I. The landing response of the fly, *Lucilia sericata*, and other Calliphorinae. *J Exp Biol* **37**, 854-878. [Journal]

Götz, K. G. (1964). Optomotorische Untersuchung des visuellen Systems einiger Augenmutanten der Fruchtfliege *Drosophila*. *Kybernetik* **2**, 77-92. [DOI: 10.1007/BF00288561]

Götz, K. G. (1968). Flight control in *Drosophila* by visual perception of motion. *Kybernetik* **4**, 199-208. [DOI: 10.1007/BF00272517]

Götz, K. G. (1975). The optomotor equilibrium of the *Drosophila* navigation system. *J Comp Physiol A Sens Neural Behav Physiol* **99**, 187-210. [DOI: 10.1007/BF00613835]

Götz, K. G. (1987). Course-control, metabolism and wing interference during ultralong tethered flight in *Drosophila melanogaster*. *J Exp Biol* **128**, 35-46. [Journal]

Götz, K. G., Hengstenberg, B. and Biesinger, R. (1979). Optomotor control of wing beat and body posture in *Drosophila*. *Biol Cybern* **35**, 101-112. [DOI: 10.1007/BF00337435]

Götz, K. G. and Wandel, U. (1984). Optomotor control of the force of flight in *Drosophila* and *Musca*. 2. Covariance of lift and thrust in still air. *Biol Cybern* **51**, 135-139. [DOI: 10.1007/BF00357927]

Grünert, U. and Gnatzy, W. (1987). Campaniform sensilla of *Calliphora vicina* (Insecta, Diptera). 2. Typology. *Zoomorphol* **106**, 320-328. [DOI: 10.1007/BF00312006]

Guest, B. B. and Gray, J. R. (2006). Responses of a looming-sensitive neuron to compound and paired object approaches. *J Neurophysiol* **95**, 1428-1441. [DOI: 10.1152/jn.01037.2005]

Haag, J. and Borst, A. (2004). Neural mechanism underlying complex receptive field properties of motion-sensitive interneurons. *Nat Neurosci* **7**, 628-634. [DOI: 10.1038/nn1245]

Harris, R. A., O'Carroll, D. C. and Laughlin, S. B. (2000). Contrast gain reduction in fly motion adaptation. *Neuron* **28**, 595-606. [DOI: 10.1016/S0896-6273(00)00136-7]

Hartline, H. K. (1934). Intensity and duration in the excitation of single photoreceptor units. *J Cell Comp Physiol* **5**, 229-247. [DOI: 10.1002/jcp.1030050210]

Hassenstein, B. and Reichardt, W. (1956). Systemtheoretische Analyse der Zeit-, Reihenfolgen- und Vorzeichenauswertung bei der Bewegungsperzeption des Russelkafers *Chlorophanus*. *Z Naturforsch B* **11**, 513-524.

Hatsopoulos, N., Gabbiani, F. and Laurent, G. (1995). Elementary computation of object approach by a wide-field visual neuron. *Science* **270**, 1000-1003. [DOI: 10.1126/science.270.5238.1000]

Heide, G. (1983). Neural mechanisms of flight control in Diptera. In *BIONA-report*, vol. 2 (ed. W. Nachtigall), pp. 35-52. Stuttgart: Fischer.

Heide, G. and Götz, K. G. (1996). Optomotor control of course and altitude in *Drosophila melanogaster* is correlated with distinct activities of at least three pairs of flight steering muscles. *J Exp Biol* **199**, 1711-1726. [Journal]

Heisenberg, M. and Wolf, R. (1979). On the fine structure of yaw torque in visual flight orientation of *Drosophila melanogaster*. *J Comp Physiol A Sens Neural Behav Physiol* **130**, 113-130. [DOI: 10.1007/BF00613749]

Heisenberg, M. and Wolf, R. (1984). *Vision in* Drosophila*: Genetics of Microbehavior*. Berlin: Springer-Verlag.

Heisenberg, M. and Wolf, R. (1988). Reafferent control of optomotor yaw torque in *Drosophila melanogaster*. *J Comp Physiol A Sens Neural Behav Physiol* **163**, 373-388. [DOI: 10.1007/BF00604013]

Higgins, C. M. (2004). Nondirectional motion may underlie insect behavioral dependence on image speed. *Biol Cybern* **91**, 326-332. [DOI: 10.1007/s00422-004-0519-x]

Jürgens, R., Becker, W. and Kornhuber, H. H. (1981). Natural and drug-induced variations of velocity and duration of human saccadic eye movements: Evidence for a control of the neural pulse generator by local feedback. *Biol Cybern* **V39**, 87-96. [DOI: 10.1007/BF00336734]

Karniel, A. (2002). Three creatures named “forward model.” *Neural Netw* **15**, 305-307. [DOI: 10.1016/S0893-6080(02)00020-5]

Kawato, M. (1999). Internal models for motor control and trajectory planning. *Curr Opin Neurobiol* **9**, 718-727. [DOI: 10.1016/S0959-4388(99)00028-8]

Kunze, P. (1961). Untersuchung des Bewegungssehens fixiert fliegender Bienen. *J Comp Physiol A Sens Neural Behav Physiol* **44**, 656-684. [DOI: 10.1007/BF00341335]

Krapp, H. G. and Hengstenberg, R. (1996). Estimation of self-motion by optic flow processing in single visual interneurons. *Nature* **384**, 463-466. [DOI: 10.1038/384463a0]

Land, M. F. (1973). Head movement of flies during visually guided flight. *Nature* **243**, 299-300. [DOI: 10.1038/243299a0]

Land, M. F. (1999). Motion and vision: Why animals move their eyes. *J Comp Physiol A Sens Neural Behav Physiol* **185**, 341-352. [DOI: 10.1007/s003590050393]

Land, M. F. and Collett, T. S. (1974). Chasing behavior of houseflies (*Fannia canicularis*) – description and analysis. *J Comp Physiol A Sens Neural Behav Physiol* **89**, 331-357. [DOI: 10.1007/BF00695351]

Laughlin, S. B. and Weckstrom, M. (1993). Fast and slow photoreceptors – a comparative study of the functional diversity of coding and conductances in the Diptera. *J Comp Physiol A Sens Neural Behav Physiol* **172**, 593-609. [DOI: 10.1007/BF00213682]

Lehmann, F.-O. and Dickinson, M. H. (1997). The changes in power requirements and muscle efficiency during elevated force production in the fruit fly *Drosophila melanogaster*. *J Exp Biol* **200**, 1133-1143. [Journal]

Lehmann, F.-O. and Dickinson, M. H. (1998). The control of wing kinematics and flight forces in fruit flies (*Drosophila* spp.). *J Exp Biol* **201**, 385-401. [Journal]

Lehmann, F.-O. and Dickinson, M. H. (2001). The production of elevated flight force compromises manoeuvrability in the fruit fly *Drosophila melanogaster*. *J Exp Biol* **204**, 627-635. [Journal]

Lehmann, F.-O. and Götz, K. G. (1996). Activation phase ensures kinematic efficacy in flight-steering muscles of *Drosophila melanogaster*. *J Comp Physiol A Sens Neural Behav Physiol* **179**, 311-322. [DOI: 10.1007/BF00194985]

Lehmann, F.-O., Sane, S. P. and Dickinson, M. (2005). The aerodynamic effects of wing-wing interaction in flapping insect wings. *J Exp Biol* **208**, 3075-3092. [DOI: 10.1242/jeb.01744]

Maimon, G. and Dickinson, M.H. (2006) Visually guided attraction and repulsion in tethered, flying *Drosophila*. *Soc Neurosci Abst* **32**:449, Atlanta, GA.

Martinez-Conde, S., Macknik, S. L. and Hubel, D. H. (2004). The role of fixational eye movements in visual perception. *Nat Rev Neurosci* **5**, 229-240. [DOI: 10.1038/nrn1348]

Mayer, M., Vogtmann, K., Bausenwein, B., Wolf, R. and Heisenberg, M. (1988). Flight control during free yaw turns in *Drosophila melanogaster*. *J Comp Physiol A Sens Neural Behav Physiol* **163**, 389-399. [DOI: 10.1007/BF00604014]

Mehta, B. and Schaal, S. (2002). Forward models in visuomotor control. *J Neurophysiol* **88**, 942-953. [Journal]

Miall, R. C. and Wolpert, D. M. (1996). Forward models for physiological motor control. *Neural Netw* 9, 1265-1279. [DOI: 10.1016/S0893-6080(96)00035-4]

Mickoleit, G. (1962). Die Thoraxmuskulatur von *Tipula vernalis* Meigen. Ein Beitrag zur vergleichenden Anatomie des Dipteranthorax. *Zool Jahrb Abt Anat Ontog Tiere* **80**, 213-244.

Morasso, P., Bizzi, E. and Dichgans, J. (1973). Adjustment of saccade characteristics during head movements. *Exp Brain Res* **V16**, 492-500. [DOI: 10.1007/BF00234475]

Nalbach, G. (1993). The halteres of the blowfly *Calliphora*. 1. Kinematics and dynamics. *J Comp Physiol A Sens Neural Behav Physiol* **173**, 293-300. [DOI: 10.1007/BF00212693]

Nalbach, G. (1994). Extremely non-orthogonal axes in a sense organ for rotation: Behavioural analysis of the dipteran haltere system. *Neurosci* **61**, 149-163. [DOI: 10.1016/0306-4522(94)90068-X]

Nalbach, G. and Hengstenberg, R. (1994). The halteres of the blowfly *Calliphora*. 2. 3-dimensional organization of compensatory reactions to real and simulated rotations. *J Comp Physiol A Sens Neural Behav Physiol* **175**, 695-708. [DOI: 10.1007/BF00191842]

Poulet, J. F. A. and Hedwig, B. (2007). New insights into corollary discharges mediated by identified neural pathways. *Trends Neurosci* **30**, 14-21. [DOI: 10.1016/j.tins.2006.11.005]

Pringle, J. W. S. (1948). The gyroscopic mechanism of the halteres of Diptera. *Phil Trans Royal Soc London B Biol Sci* **233**, 347-384. [JSTOR]

Pringle, J. W. S. (1949). The excitation and contraction of the flight muscles of insects. *J Physiol* **108**, 226-232. [PubMed]

Ramat, S., Leigh, R. J., Zee, D. S. and Optican, L. M. (2007). What clinical disorders tell us about the neural control of saccadic eye movements. *Brain* **130**, 10-35. [DOI: 10.1093/brain/awl309]

Reichardt, W. (1961). Autocorrelation, a principle for relative movement discrimination by the central nervous system. In *Sensory Communication*, (ed. W. Rosenblith), pp. 303-317. New York: MIT Press.

Reichardt, W. (1969). Movement perception in insects. In *Processing of Optical Data by Organisms and Machines*, (ed. W. Reichardt), pp. 465-493. New York, London: Academic Press.

Reichardt, W. (1973). Musterinduzierte Flugorientierung der Fliege *Musca domestica*. *Naturwissenschaften* **60**, 122-138. [DOI: 10.1007/BF00594781]

Reichardt, W., Egelhaaf, M. and Guo, A. K. (1989). Processing of figure and background motion in the visual system of the fly. *Biol Cybern* **61**, 327-345. [DOI: 10.1007/BF00200799]

Reichardt, W. and Poggio, T. (1976). Visual control of orientation behavior in the fly. 1. A quantitative analysis. *Q Rev Biophys* **9**, 311-375. [Medline]

Reichardt, W. and Poggio, T. (1979). Figure-ground discrimination by relative movement in the visual system of the fly. I. Experimental results. *Biol Cybern* **35**, 81-100. [DOI: 10.1007/BF00337434]

Reiser, M. B. (2006). Visually mediated control of flight in *Drosophila*. Ph.D. thesis, California Institute of Technology, Pasadena. [Caltech Libraries]

Sandeman, D. C. (1980). Angular acceleration, compensatory head movements and the halteres of flies (*Lucilia serricata*). *J Comp Physiol A Sens Neural Behav Physiol* **136**, 361-367. [DOI: 10.1007/BF00657358]

Sandeman, D. C. and Markl, H. (1980). Head movements in flies (*Calliphora*) produced by deflection of the halteres. *J Exp Biol* **85**, 43-60. [Journal]

Santer, R. D., Simmons, P. J. and Rind, F. C. (2005). Gliding behaviour elicited by lateral looming stimuli in flying locusts. *J Comp Physiol A Neuroethol Sens Neural Behav Physiol* **191**, 61-73. [DOI: 10.1007/s00359-004-0572-x]

Schilstra, C. and van Hateren, J. H. (1999). Blowfly flight and optic flow. I. Thorax kinematics and flight dynamics. *J Exp Biol* **202**, 1481-1490. [Journal]

Sellke, K. (1936). Biologische und morphologische Studien an schädlichen Wiesenschnacken (Tipulidae, Dipt). *Z Wissensch Zool* **148**, 465-555.

Sherman, A. and Dickinson, M. H. (2003). A comparison of visual and haltere-mediated equilibrium reflexes in the fruit fly *Drosophila melanogaster*. *J Exp Biol* **206**, 295-302. [DOI: 10.1242/jeb.00075]

Sherman, A. and Dickinson, M. H. (2004). Summation of visual and mechanosensory feedback in *Drosophila* flight control. *J Exp Biol* **207**, 133-142. [DOI: 10.1242/jeb.00731]

Sperry, R. W. (1950). Neural basis of the spontaneous optokinetic response produced by visual inversion. *J Comp Physiol Psychol* **43**, 482-489. [Medline]

Stark, W. S. and Johnson, M. A. (1980). Microspectrophotometry of *Drosophila* visual pigments: Determinations of conversion efficiency in r1–6 receptors. *J Comp Physiol A Sens Neural Behav Physiol* **140**, 275-286. [DOI: 10.1007/BF00606268]

Strausfeld, N. J. and Seyan, H. S. (1985). Convergence of visual, haltere, and prosternal inputs at neck motor neurons of *Calliphora erythrocephala*. *Cell Tissue Res* **240**, 601-615. [DOI: 10.1007/BF00216350]

Sun, H. J. and Frost, B. J. (1998). Computation of different optical variables of looming objects in pigeon nucleus rotundus neurons. *Nat Neurosci* **1**, 296-303. [DOI: 10.1038/1110]

Tammero, L. F. and Dickinson, M. H. (2002a). Collision-avoidance and landing responses are mediated by separate pathways in the fruit fly, *Drosophila melanogaster*. *J Exp Biol* **205**, 2785-2798. [Journal]

Tammero, L. F. and Dickinson, M. H. (2002b). The influence of visual landscape on the free flight behavior of the fruit fly *Drosophila melanogaster*. *J Exp Biol* **205**, 327-343. [Journal]

Tammero, L. F., Frye, M. A. and Dickinson, M. H. (2004). Spatial organization of visuomotor reflexes in *Drosophila*. *J Exp Biol* **207**, 113-122. [DOI: 10.1242/jeb.00724]

Thomas, J. B. and Wyman, R. J. (1984). Mutations altering synaptic connectivity between identified neurons in *Drosophila*. *J Neurosci* **4**, 530-538. [Journal]

Trimarchi, J. R. and Murphey, R. K. (1997). The *shaking-B*^{2} mutation disrupts electrical synapses in a flight circuit in adult *Drosophila*. *J Neurosci* **17**, 4700-4710. [Journal]

Tu, M. S. and Dickinson, M. H. (1996). The control of wing kinematics by two steering muscles of the blowfly (*Calliphora vicina*). *J Comp Physiol A Sens Neural Behav Physiol* **178**, 813-830. [DOI: 10.1007/BF00225830]

van Hateren, J. H. and Schilstra, C. (1999). Blowfly flight and optic flow. II. Head movements during flight. *J Exp Biol* **202**, 1491-1500. [Journal]

van Opstal, A. J. and Kappen, H. (1993). A two-dimensional ensemble coding model for spatial-temporal transformation of saccades in monkey superior colliculus. *Network Comp Neural Sys* **4**, 19-38. [DOI: 10.1088/0954-898X/4/1/003]

Virsik, R. and Reichardt, W. (1974). Tracking of moving objects by the fly *Musca domestica*. *Naturwissenschaften* **61**, 132-133. [DOI: 10.1007/BF00606295]

Virsik, R. P. and Reichardt, W. (1976). Detection and tracking of moving objects by the fly *Musca domestica*. *Biol Cybern* **23**, 83-98. [DOI: 10.1007/BF00336012]

Vogel, S. (1966). Flight in *Drosophila*: I. Flight performance of tethered flies. *J Exp Biol* **44**, 567-578. [Journal]

Vogel, S. (1967). Flight in *Drosophila*: II. Variations in stroke parameters and wing contour. *J Exp Biol* **46**, 383-392. [Journal]

von Buddenbrock, W. (1919). Die vermutliche Lösung der Halterenfrage. *Pflügers Archiv Europ J Physiol* **175**, 125-164. [DOI: 10.1007/BF01722145]

von Holst, E. and Mittelstaedt, H. (1950). Das Reafferenzprinzip (Wechselwirkungen zwischen Zentralnervensystem und Peripherie). *Naturwissenschaften* **37**, 464-476. [DOI: 10.1007/BF00622503]

Wagner, H. (1986). Flight performance and visual control of flight of the free-flying housefly (*Musca domestica* L.) II. Pursuit of targets. *Phil Trans Royal Soc London B Biol Sci* **312**, 553-579. [JSTOR]

Walls, G. L. (1962). The evolutionary history of eye movements. *Vision Res* **2**, 69-80.

Webb, B. (2004). Neural mechanisms for prediction: Do insects have forward models? *Trends Neurosci* **27**, 278-282. [DOI: 10.1016/j.tins.2004.03.004]

Weis-Fogh, T. (1973). Quick estimates of flight fitness in hovering animals, including novel mechanisms for lift production. *J Exp Biol* **59**, 169-230. [Journal]

Wicklein, M. and Strausfeld, N. J. (2000). Organization and significance of neurons that detect change of visual depth in the hawk moth *Manduca sexta*. *J Comp Neurol* **424**, 356-376. [DOI: 10.1002/1096-9861(20000821)424:2<356::AID-CNE12>3.0.CO;2-T]

Wolf, R. and Heisenberg, M. (1990). Visual control of straight flight in *Drosophila melanogaster*. *J Comp Physiol A Sens Neural Behav Physiol* **167**, 269-283. [DOI: 10.1007/BF00188119]

Yarbus, A. L. (1961). Движение глаз при наблюдении сложных объектов. *Биофизика* **6**, 52-56. [Medline]

Yarbus, A. L. (1967). *Eye Movements and Vision*. New York: Plenum.